Monochromatic X-ray sources based on Table-top electron accelerators and X-ray tubes

A.P. Potylitsyn
TPU, Tomsk, Russia

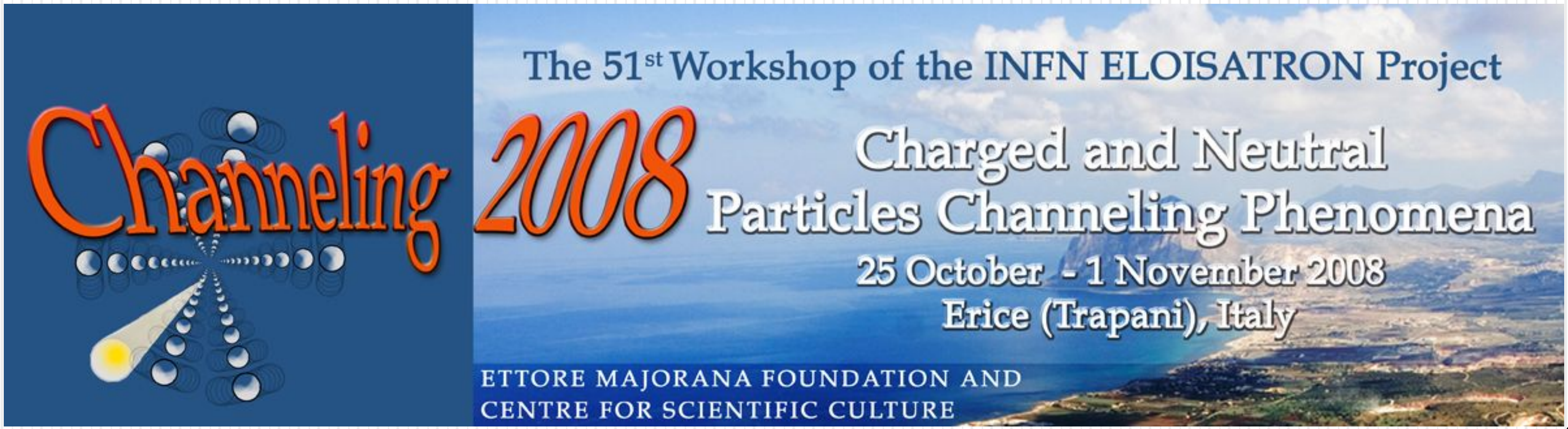

The main radiation mechanisms in amorphous targets:

- Bremsstrahlung
- Transition radiation

In order to obtain a monochromatic source one should use monochromator

Other targets allow to obtain quasi-monochromatic lines in spectrum:

- Multilayer targets (RTR)
- Crystals (CBS, channeling radiation, PXR)

Monochromatic X-ray source based on X-ray tube

Monochromatic X-ray source for calibrating X-ray telescopes. V. Arkadiev, H. Brauninger, W. Burkert, A. Bzhaumikhov, H.-E. Gorny, N. Langhoff*, A. Oppitz, J. Rabe.* Nuclear Instruments and Methods in Physics Research A 455 (2000) 589-595

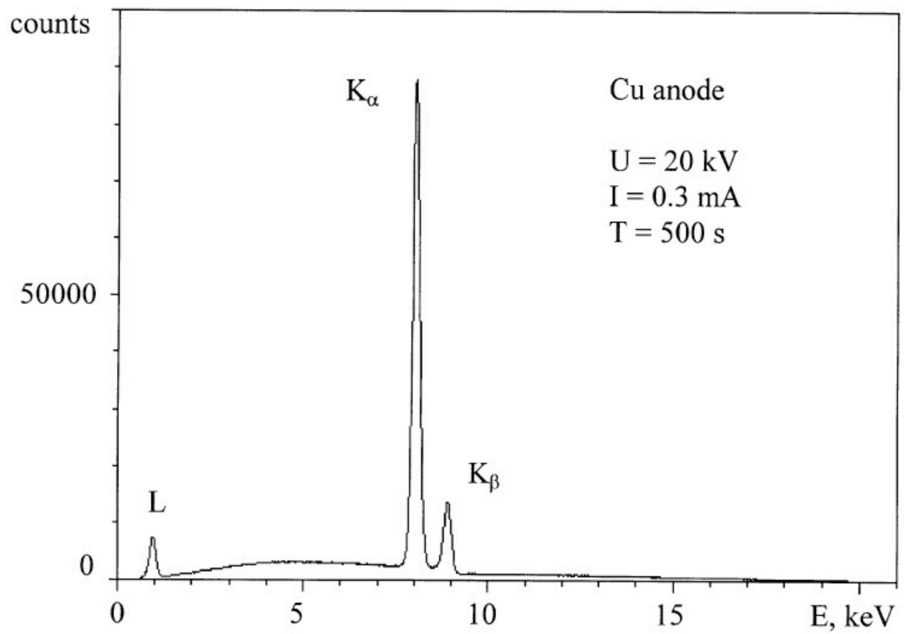

Measured spectrum of the X-ray tube with a Cu anode.

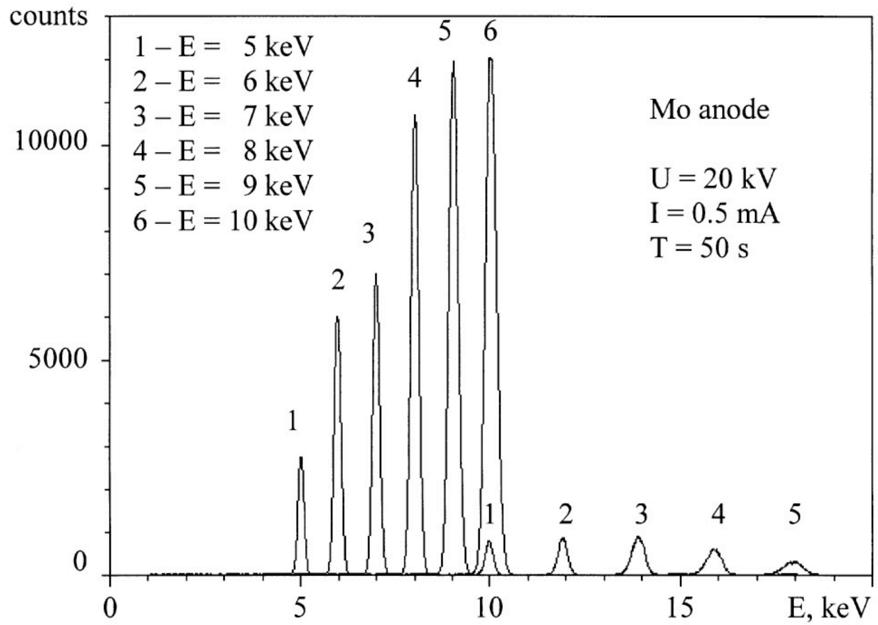

Measured spectra with the HOPG crystals (first and second reflection orders).

$$\Delta E/E \sim 3 \div 4\%$$

Monochromatic γ-ray source based on accelerator

First results of the tunable monochromatic gamma-ray source at the Ghent 15 MeV Linac. M. Berschy, M. Crittin, J. Jolie, N. Warr, W. Mondelaers.
NIM B 99 (1995), pp. 286-288

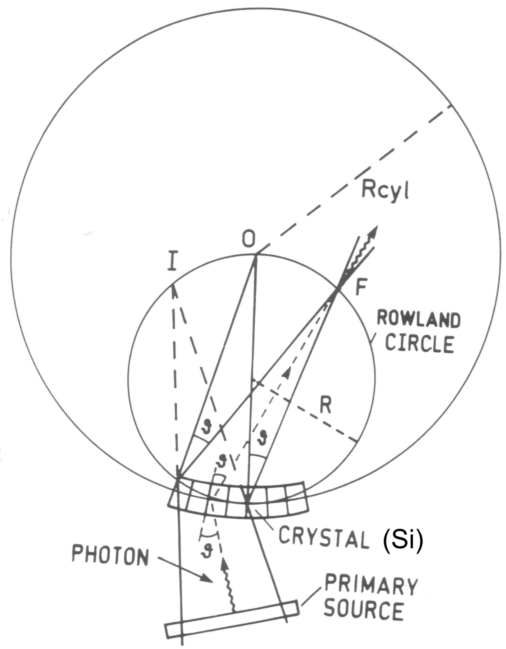

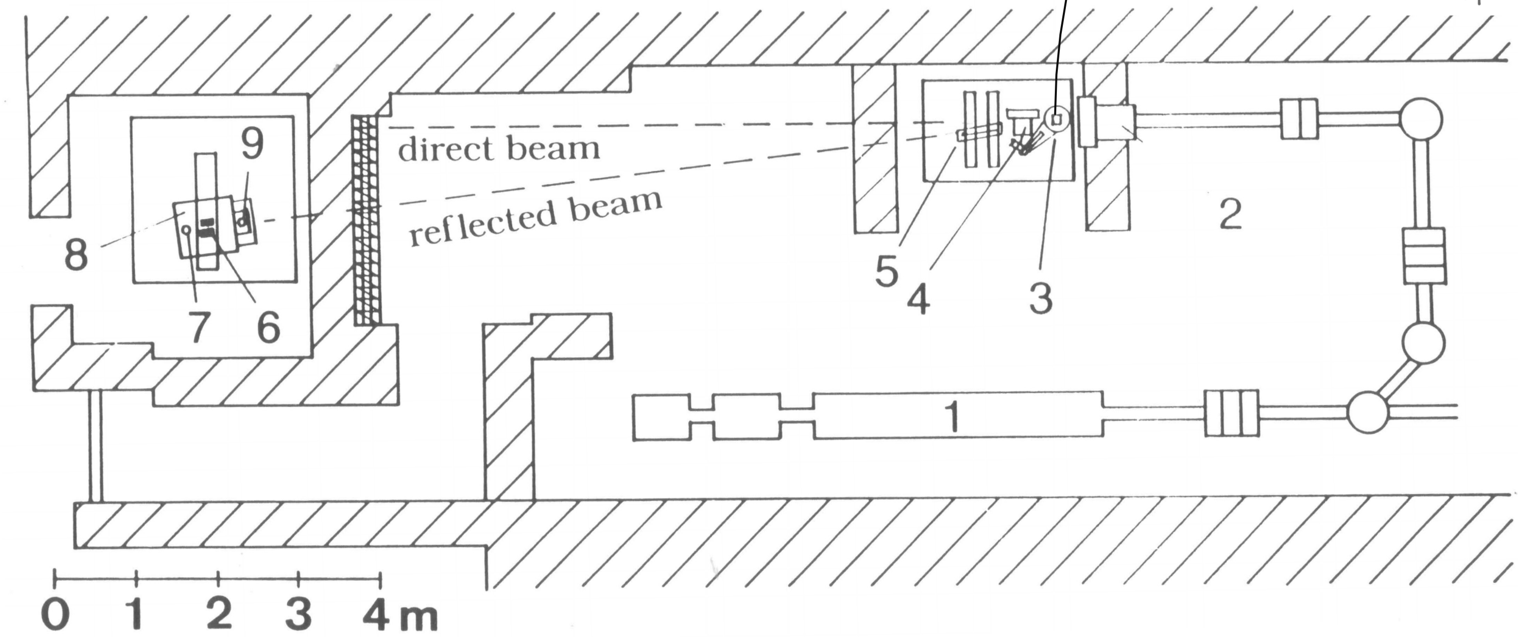

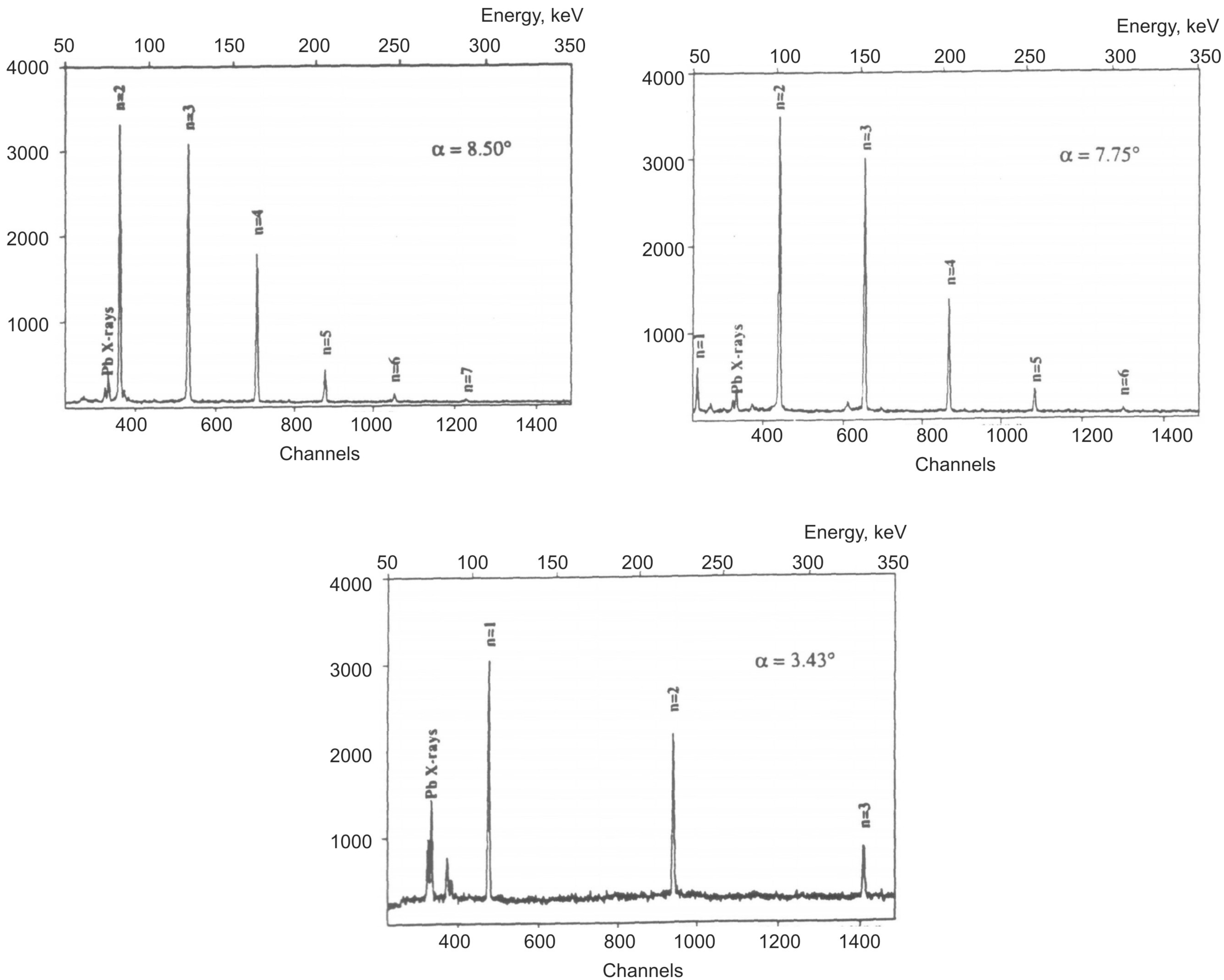

Energy, keV
50 100 150 200 250 300 350
4000 3000 2000 1000
α = 8.50°
Pb X-rays
n=2
n=3
n=4
n=5
n=6
n=7
400 600 800 1000 1200 1400
Channels
Energy, keV
50 100 150 200 250 300 350
4000 3000 2000 1000
α = 7.75°
n=1
Pb X-rays
n=2
n=3
n=4
n=5
n=6
400 600 800 1000 1200 1400
Channels
Energy, keV
50 100 150 200 250 300 350
4000 3000 2000 1000
α = 3.43°
Pb X-rays
n=1
n=2
n=3
400 600 800 1000 1200 1400
Channels

X-ray source based on RTR

Observation of soft x rays of single-mode resonant transition radiation from a multilayer target with a submicrometer period. Koji Yamada and Teruo Hosokawa, Hisataka Takenaka. Physical Review A V. 59, № 5 (1999)

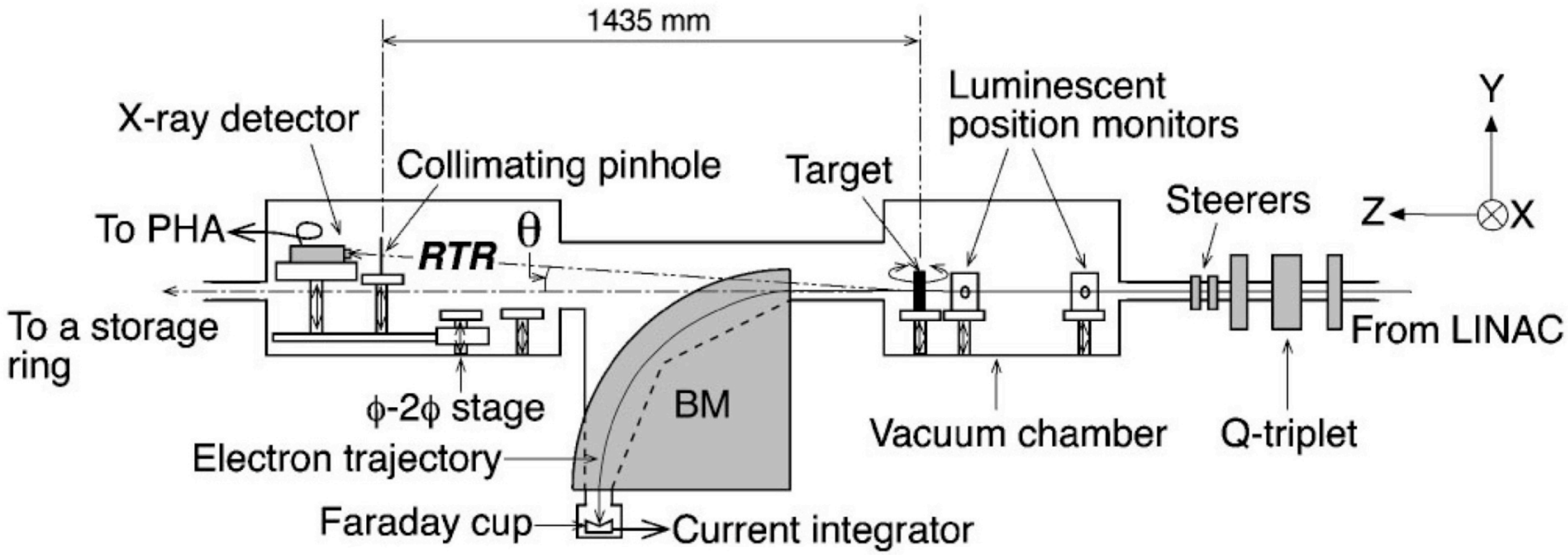

Experimental setup for RTR measurement.

Schematic of the resonance effect of TR in a multilayer target.

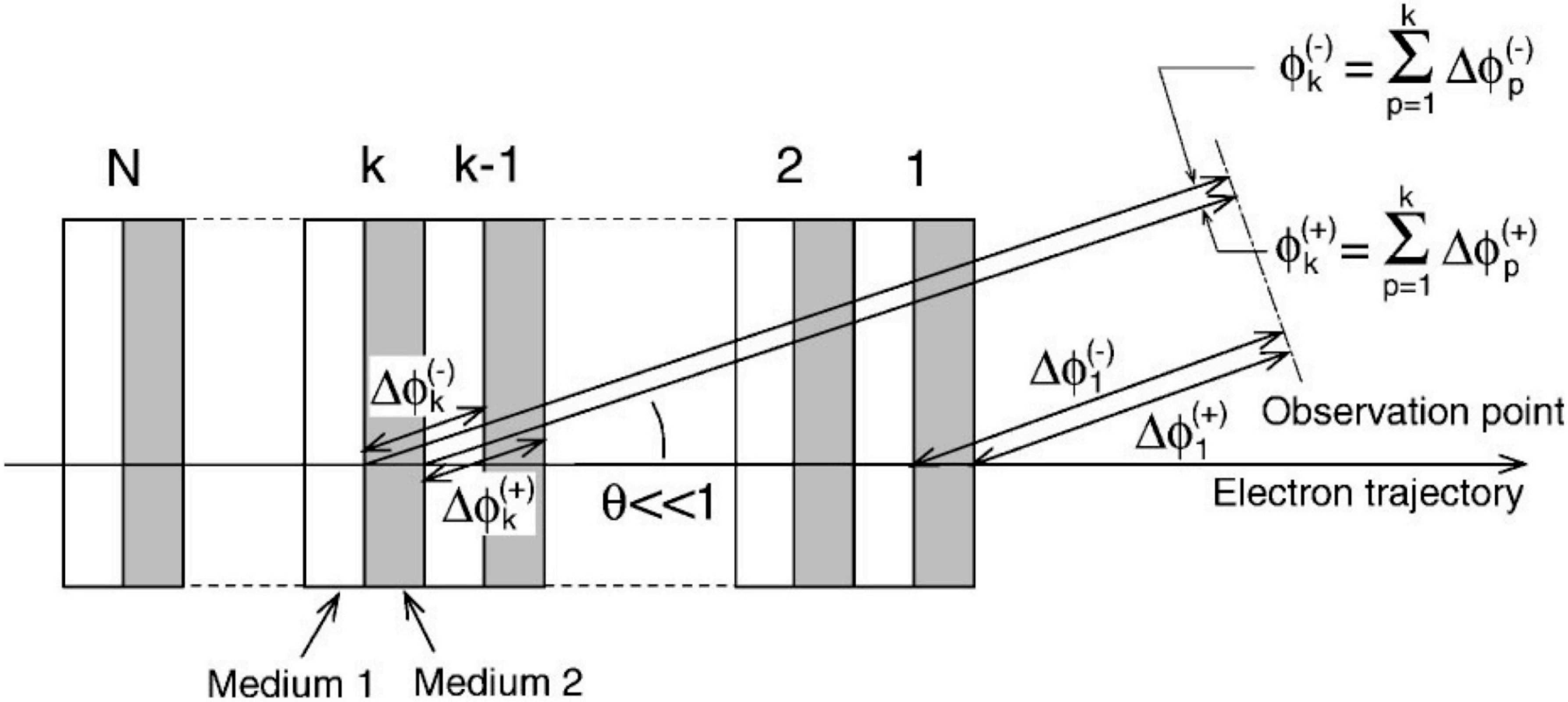

Ni/C multilayer target.

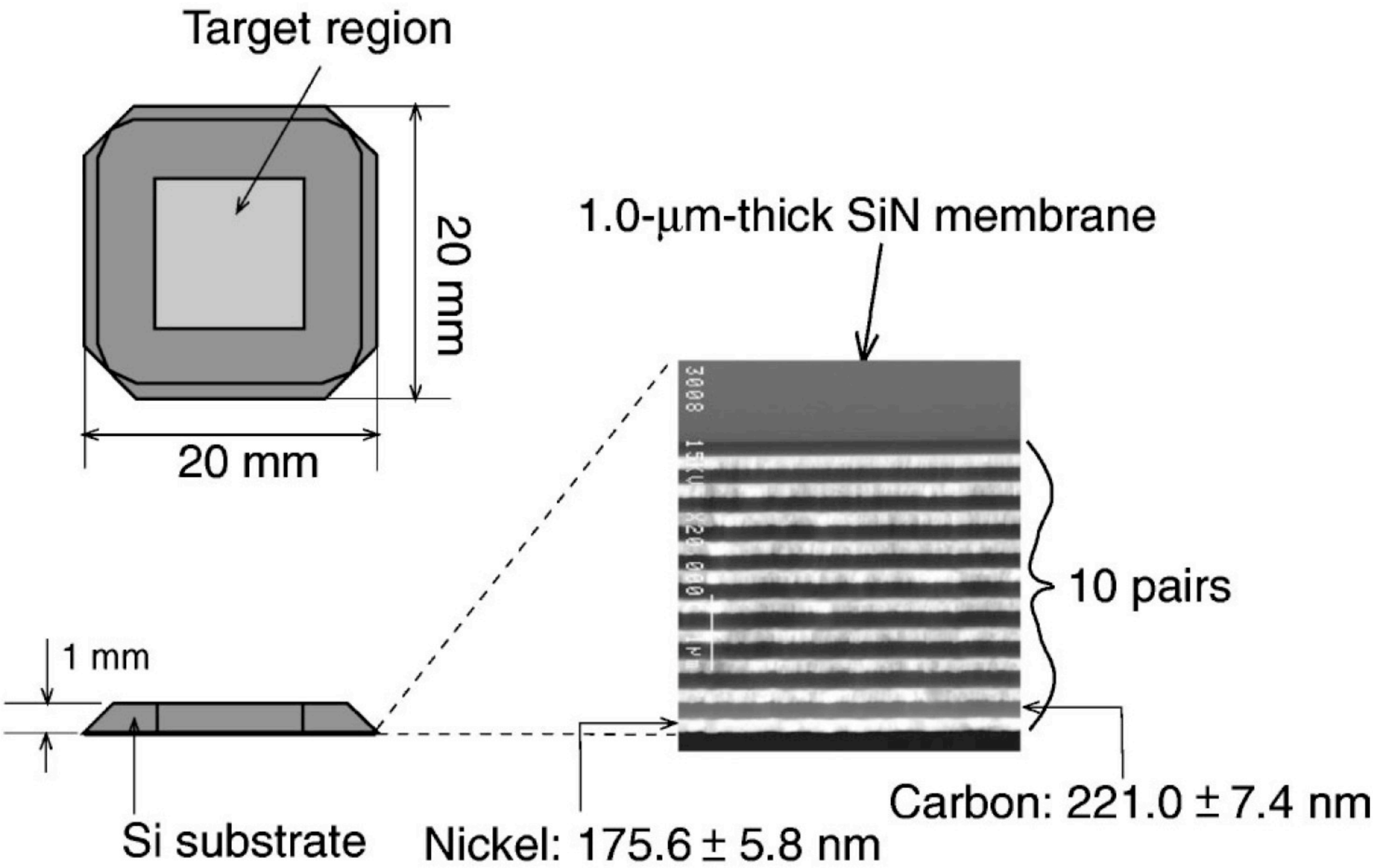

An example of the raw data of the RTR spectrum measurements.

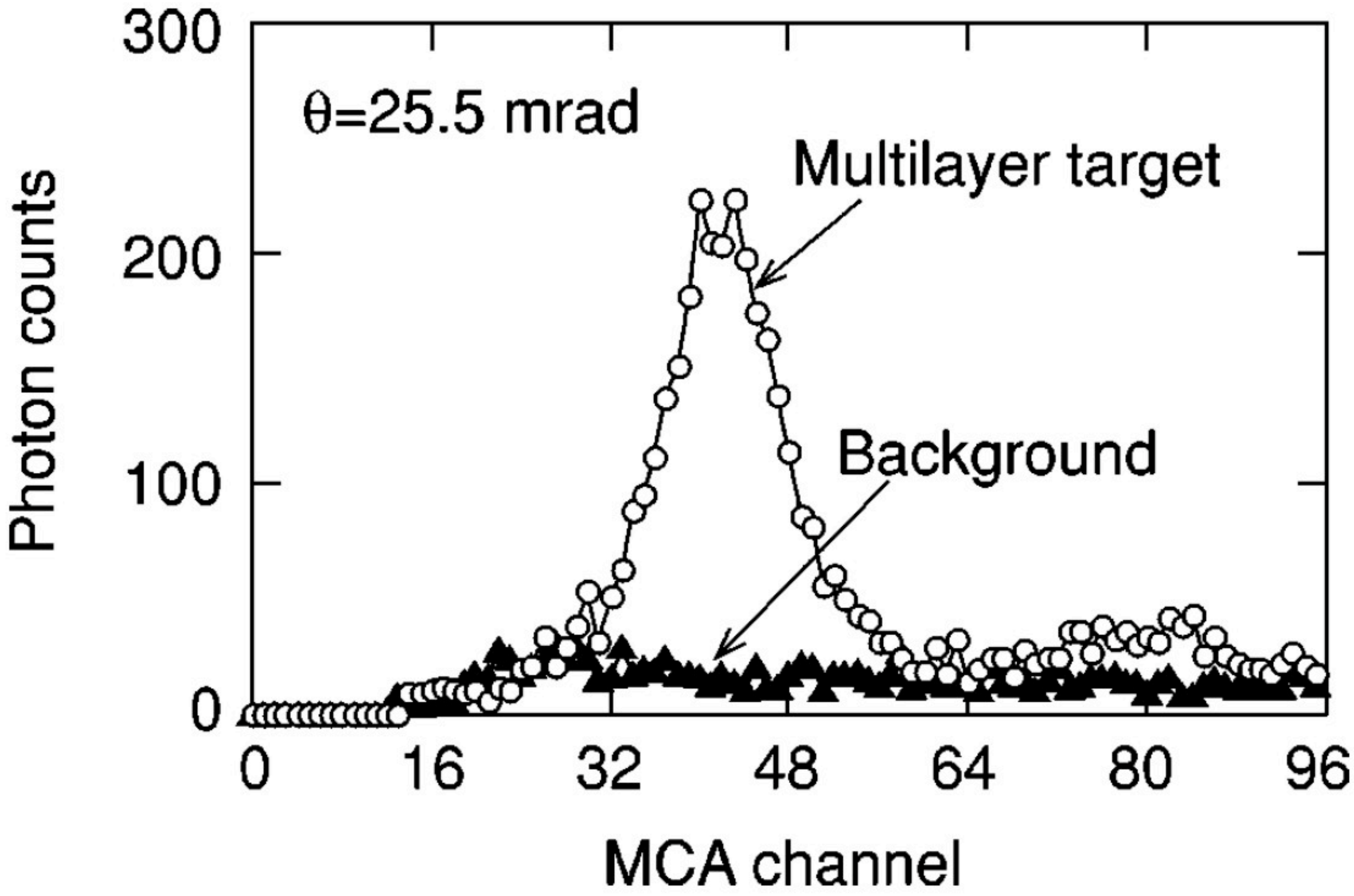

Measured RTR spectra. The open circles and solid lines represent the experimental photon yields and their fitted Gaussian functions, respectively. The dotted lines represent the spectra of theoretical estimations. The error bars are not shown in these figures because their sizes are almost the same as that of the symbols.

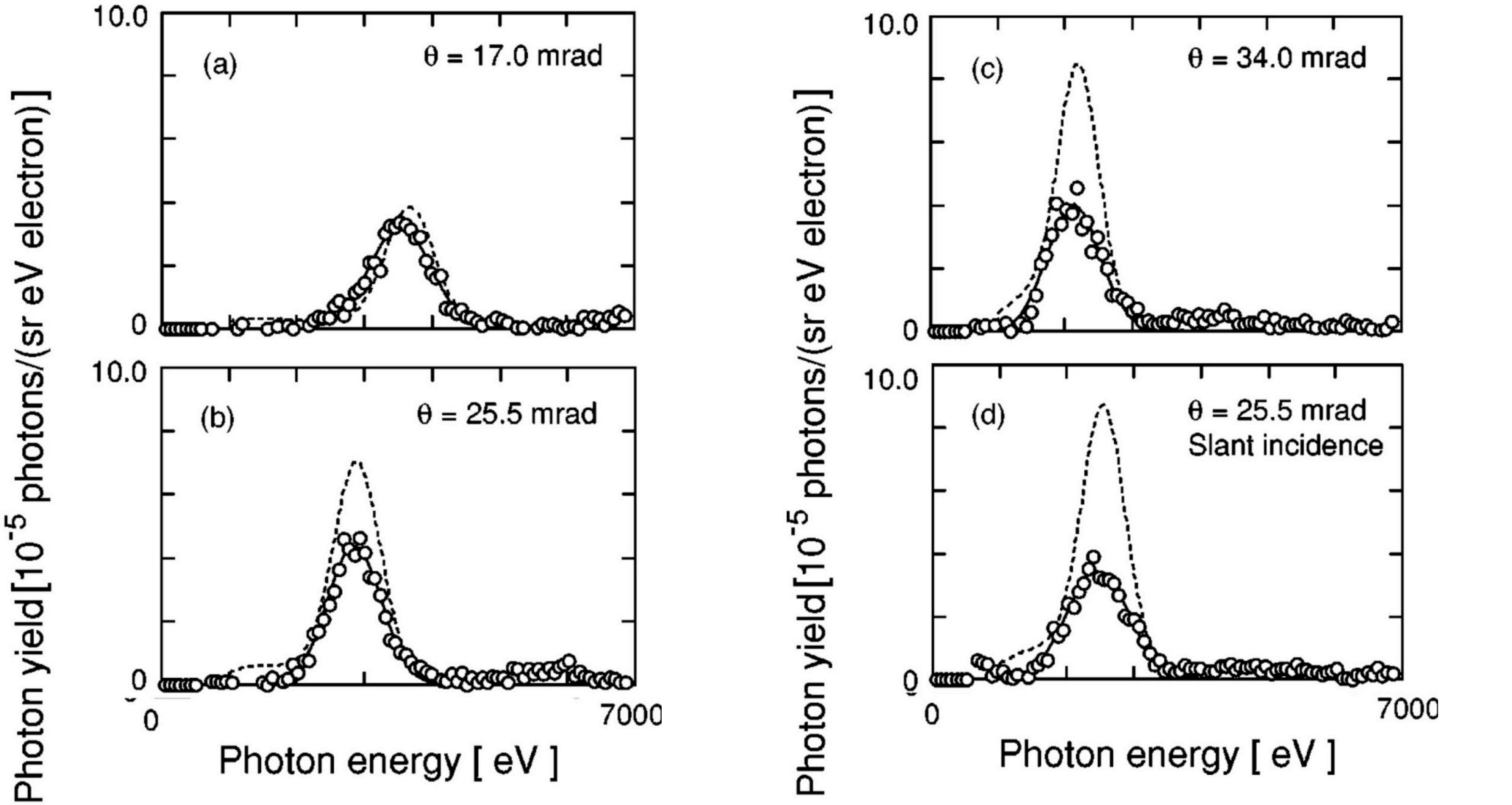

Comparison of TR and Bremsstrahlung (BS)

Parametric X-ray radiation, transition radiation and bremsstrahlung in X-ray region. A comparative Analysis. A.P. Potylitsyn and I.E. Vnukov. Electron-photon interaction in dense media. Ed.Helmut Wiedemann, Kluwer Academic Publishers, 2002.

Bremsstrahlung from a thin target

$$\frac{dW}{d\omega d\Omega} = \omega \frac{d\sigma}{d\omega d\Omega}$$
$$= \frac{2z^2\alpha^3}{\pi}\frac{\gamma^2}{(1+u^2)^4}\{[1+(1-x)^2](1+u^2)^2(2\Gamma+3) - 2(1-x)(1+u^2)^2$$
$$- 8(1-x)u^2\Gamma\}$$

Here z is the charge; α is the fine-structure constant; γ is the Lorentz factor,

$x = \omega/E$, *ω, E* are the energies of a photon and the initial electron;

u=*γθ*, *θ* is the angle of outgoing photon;

$$\Gamma = \ln\frac{1+u^2}{\lambda} - 2 \qquad\qquad \lambda = z^{1/3}/111$$

$$\frac{dW}{d\omega d\Omega} \approx const\,\frac{1+u^4}{(1+u^2)^4}$$

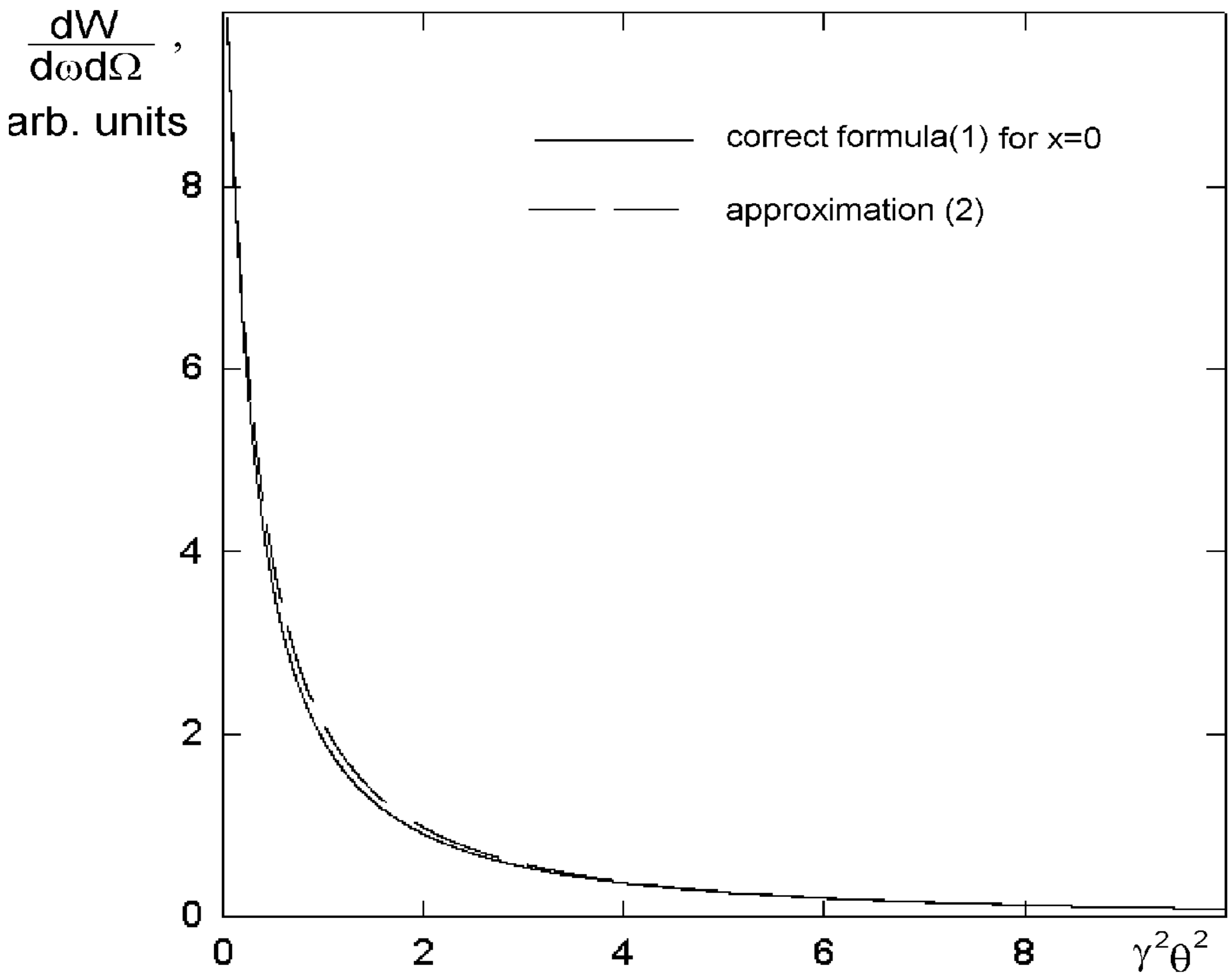

Angular distribution of BS

$$\frac{dW^{\circ}_{BS}}{d\omega} = \int \frac{dW^{\circ}_{BS}}{d\omega d\Omega} d\,\Omega = \frac{l_t}{L_{rad}} = const \qquad W^{\circ}_{BS} = \int_0^E \frac{dW^{\circ}_{BS}}{d\omega} dE = \frac{l_t}{L_{rad}} E$$

$$\frac{dW_{BS}}{d\omega d\Omega} = \frac{3}{2\pi} \frac{l_t}{L_{rad}} \gamma^2 \frac{1+u^4}{(1+u^2)^2 \left(1+u^2+\left(\frac{\gamma\omega_p}{\omega}\right)^2\right)^2}$$

Transition radiation from a single foil

Transition radiation from the foil with thickness l_t

$$\frac{dW_{TR}}{d\omega d\Omega} = \frac{\alpha}{\pi^2}\gamma^2 u^2 \left[\frac{1}{1+u^2+\left(\frac{\gamma\omega_p}{\omega}\right)^2} - \frac{1}{1+u^2}\right]^2 \left|1 - exp\left(i\frac{l_t}{l_f}\right)\right|^2$$

The formation length l_f

$$l_f = \frac{\gamma^2\lambda}{1+u^2+\left(\frac{\gamma\omega_p}{\omega}\right)^2} = \frac{2\pi}{\omega}\frac{\gamma^2}{1+u^2+\left(\frac{\gamma\omega_p}{\omega}\right)^2}$$

$$\frac{dW_{TR}}{d\omega} = \int_0^{2\pi} d\varphi \int_0^{\theta_c} \theta d\theta \frac{dW_{TR}}{d\omega d\Omega} = \frac{2\alpha}{\pi}\left[\left(1+\frac{2}{k_0^2}\right)\ln\frac{(1+k_0^2)(1+u_c^2)}{1+u_c^2+k_0^2} - \frac{u_c^2(2+k_0^2+2u_c^2)}{(1+u_c^2)(1+u_c^2+k_0^2)}\right]$$

Here $k_0^2 = \frac{\gamma^2\omega_p^2}{\omega^2}$

$$\Delta N_{ph} = \frac{dW}{d\omega}\frac{\Delta\omega}{\omega}$$

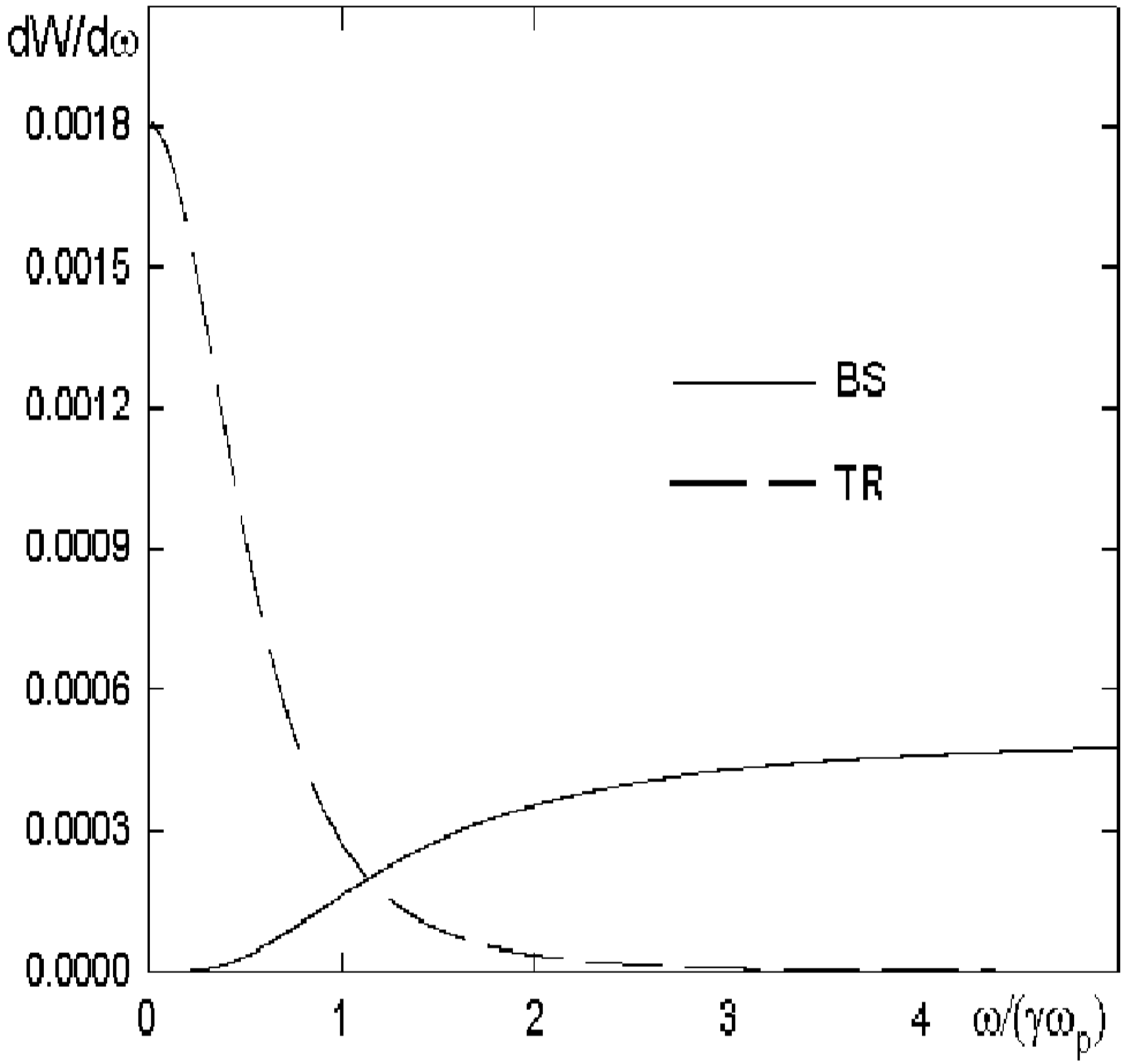

Spectral distribution of TR from single foil with $l_t \ll l_f$ (dashed curve) and BS from target $l_t = 10^{-3} L_{rad}$ (solid curve). Collimation angle $\theta_c = \gamma^{-1}$.

Optimization of transition radiation emitting targets for storage ring synchrotrons used as X-Ray lithography source. D.Minkov, H. Yamada, N. Toyosugi, T. Yamaguchi, T.Kadono, M. Morita. Applied Physics B 86, 19-23 (2007)

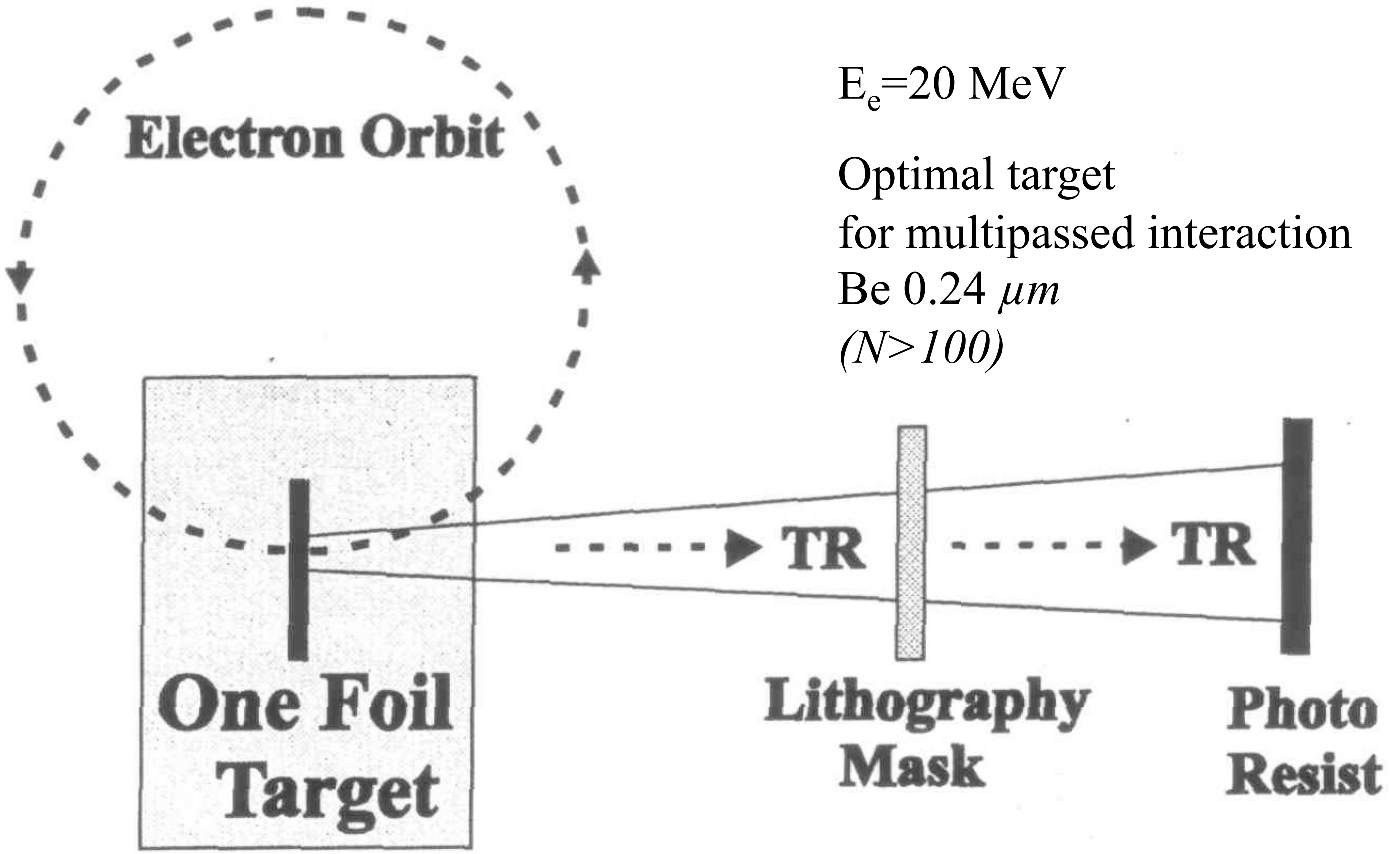

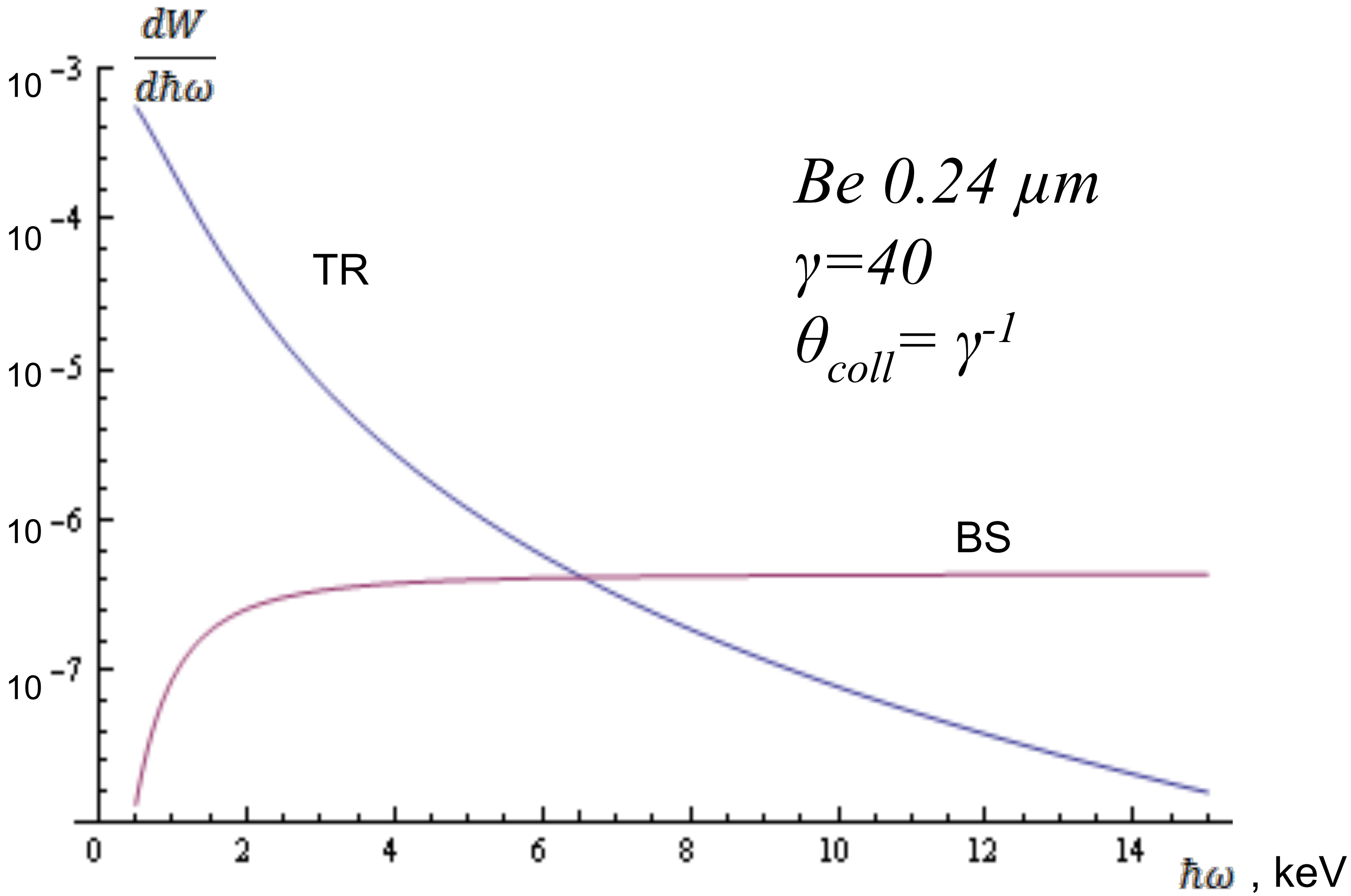

Spectral distribution of TR and BS from thin Be target

Parametric X-ray sources

A.R. Wagner, A.P.Potylitsyn, et al., Monochromatic X-ray sources based on a mechanism of real and virtual photons diffraction in crystals, NIM **B** 266 (2008) 3893 - 3897

EXPERIMENTAL LAYOUT

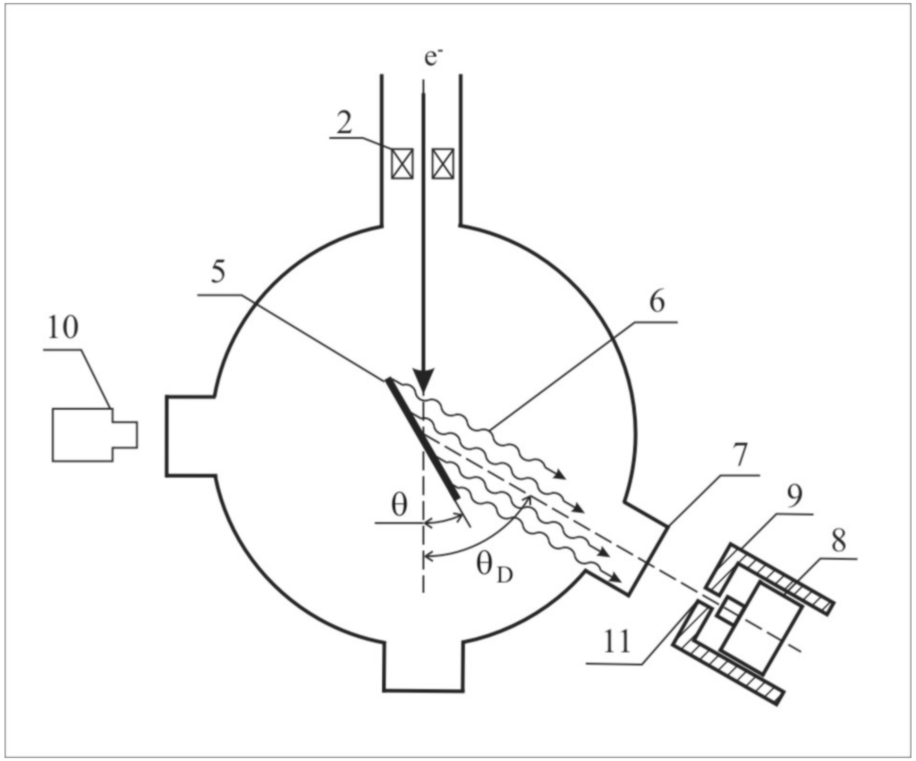

2 is current sensor, 5 is pyrolytic graphite crystal C(002) fixed on goniometer, 6 is diffractions X-ray radiation, 7 is kapton window (150 μm),
8 is semiconductor silicon detector with a sensitivity region about 13 mm^2,
9 is lead chamber, 10 is TV-camera, 11 is collimator

EXPERIMENTAL LAYOUT

Parameters of electron beam		
Parameters	value	unit
Electron energy	5.7±0.02	MeV
Cross-section size of electron beam	2.50	mm
Current electron beam	0.15-0.30	mA
Impulse time	0.60	μs
Frequency	25	Hz

Parameters of pyrolitic graphite crystal C (002)		
Parameters	value	unit
Thickness	350	μm
Mosaicisity	4	mrad

RESULTS OF EXPERIMENT

Parametric X-ray radiation

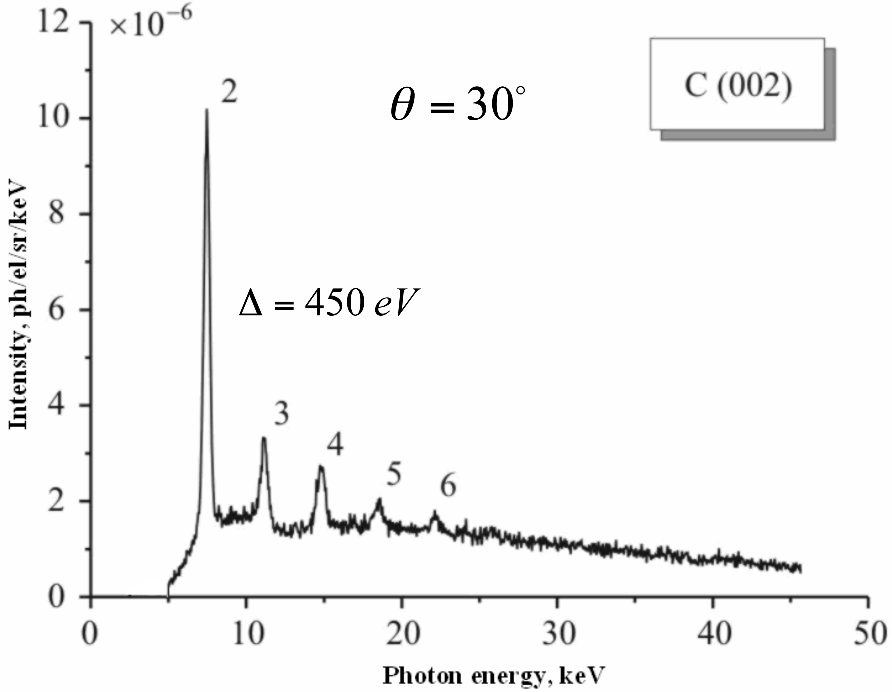

Spectrum of PXR

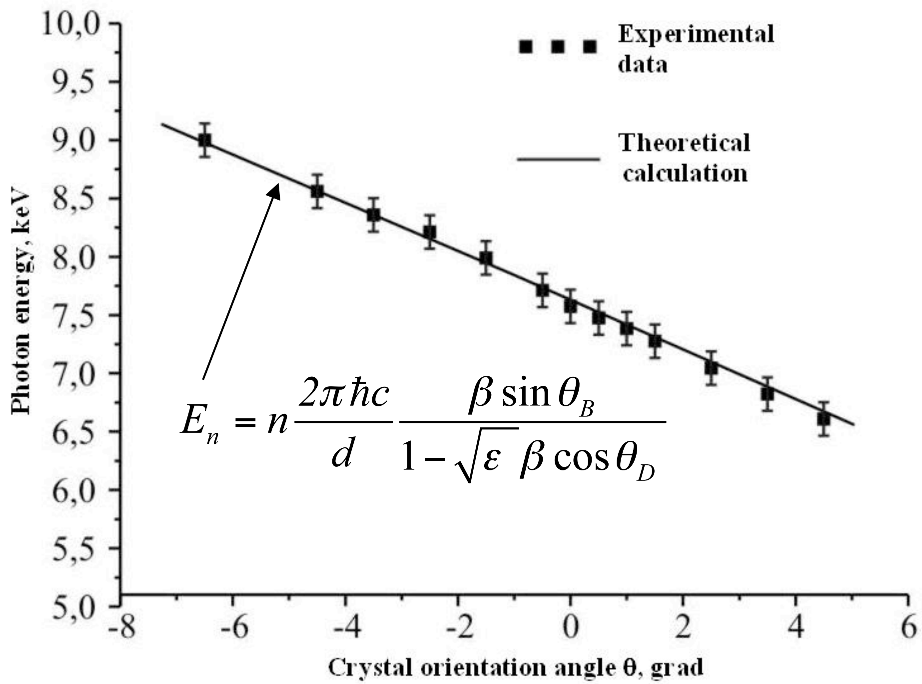

Angular distribution of PXR
for second diffraction order

$8\cdot10^{-6}$ ph/e⁻/sr

Global plane effect of PXR

Kinematic grouping of reflections of parametric X-ray radiation. A.S. Gogolev, A.P. Potylitsyn and S.R. Uglov. Journal of surface investigation. X-ray, synchrotron neutron techniques 2008. vol. 2, №2, pp. 217-224

- Superposition of all reflections of PXR, when spectral lines of each reflection is located near isolated position on energy scale.

- As in the case of plane effect (arrange effect for relativistic particles) *) the following condition is needed:
- $\mathbf{g}_i \cdot \mathbf{v}$=const, i=1,2,…
- It is sufficient to guide particle along direction <111>, in order to prove given condition for all reflections of PXR.

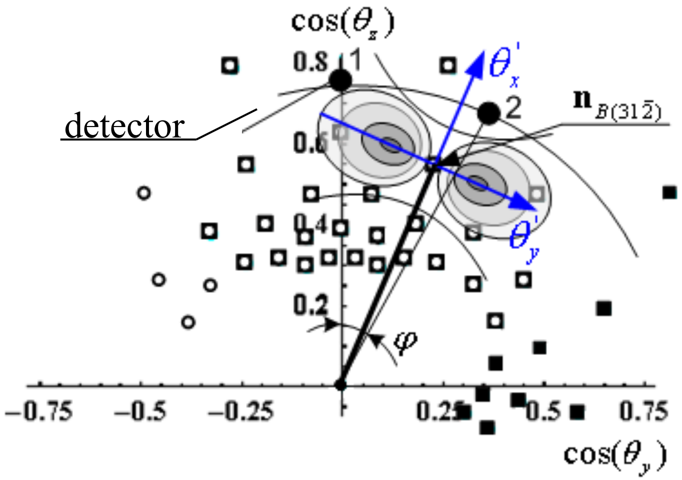

Diagram of Bragg's directions from tungsten crystal (111) in lab coordinates with Lorentz-factor 12, beam is guided along axis OX (<111>).
○ – reflections which make investment for detector's position № 1,
■ – reflections which make investment for detector's position № 2, [?] = 30°

- * Shchagin A.V., Pristupa V.I., Khizhnyak N.A. Phys.Lett. A. 148 (1990) 485-488

Simulation results

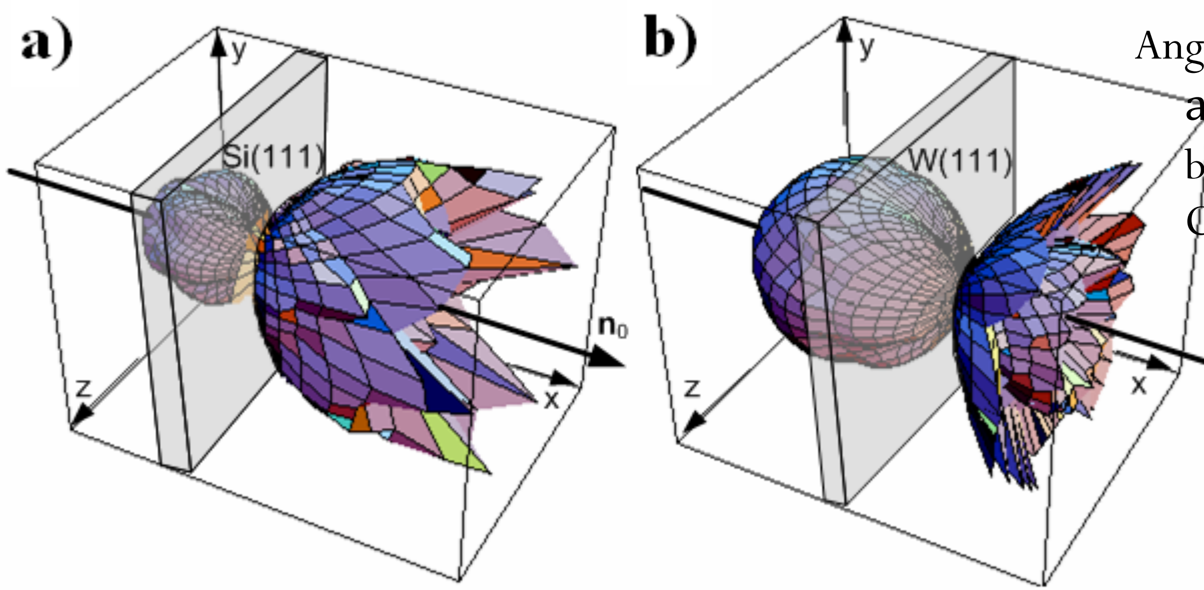

Angular distribution of PXR [illegible] = 3:

a) silicon (111) 100 μm;

b) tungsten(111) 100 μm.

Crystal is transverse to beam (the bigger side of the crystal is parallel to crystallographic planes (111))

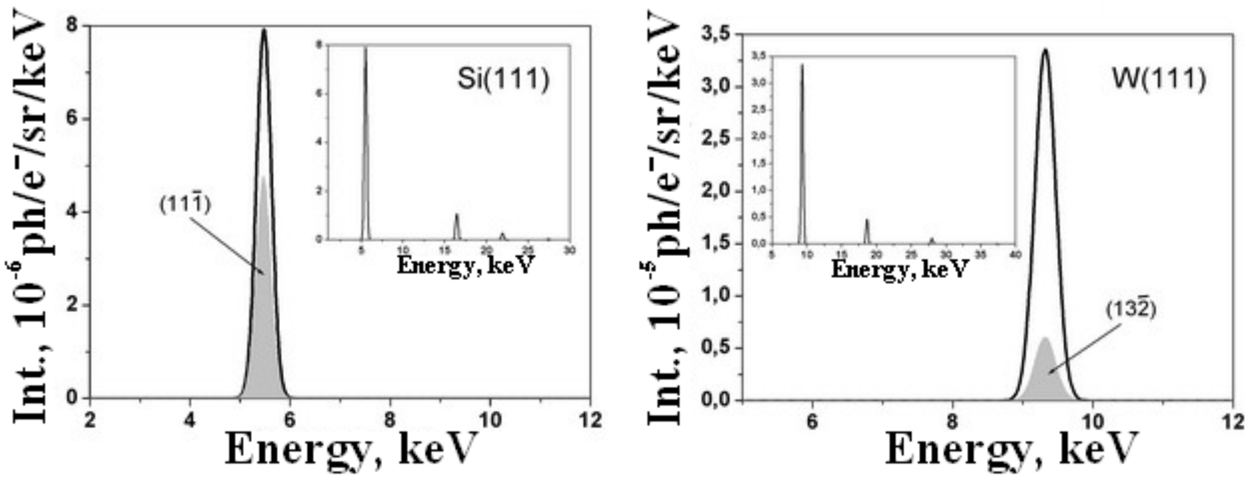

Observation angle is relative to beam's axis : in case of Si 35°, multiplication 150%; in case of W 55°, multiplication 456%. (theoretical case)

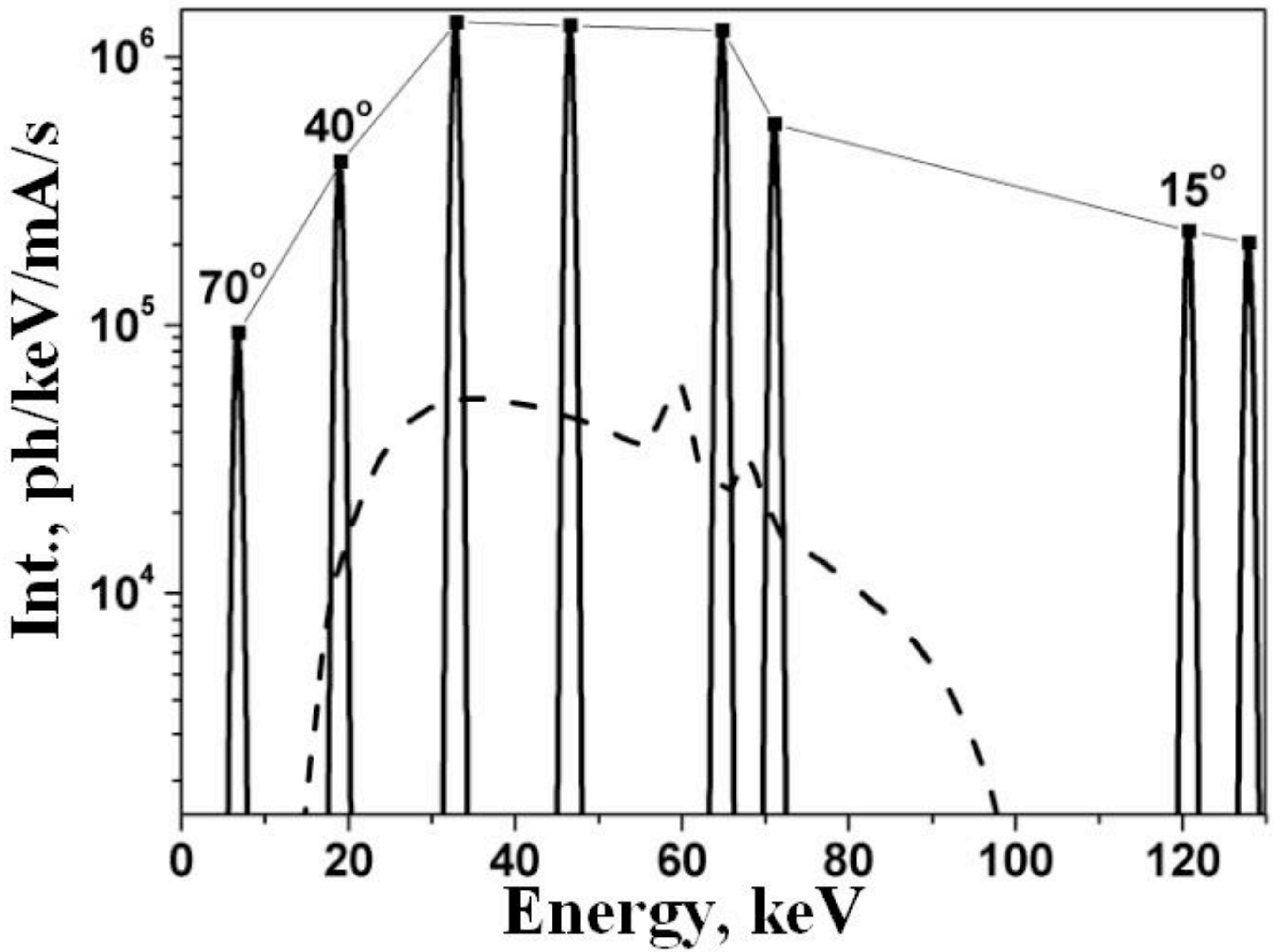

Position dependence of PXR line on observation angle.

Dashed curve – spectrum of radiation of X-ray tube with tungsten anode (130 kV)

PXR in tungsten crystal with moderately relativistic carbon nucleus(γ=3.13)

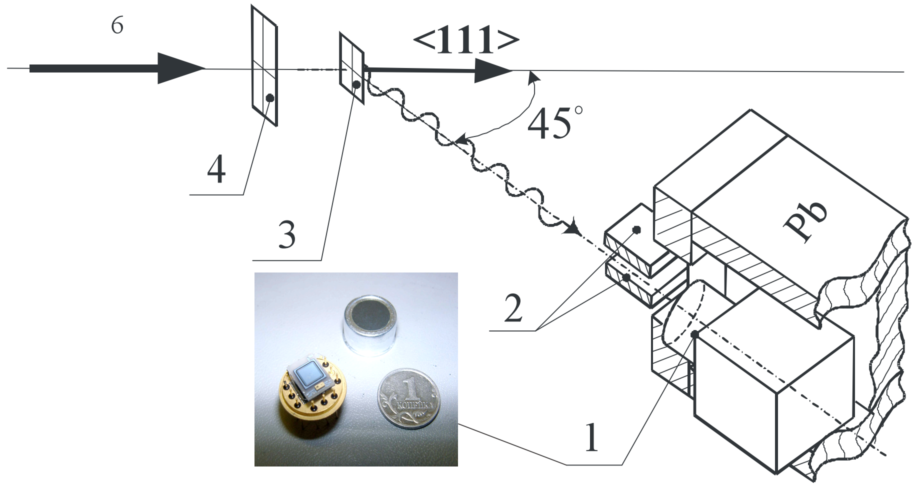

Fig. 1. Experimental scheme :
1-detector;
2-magnits;
3-target;
4-ionization chamber

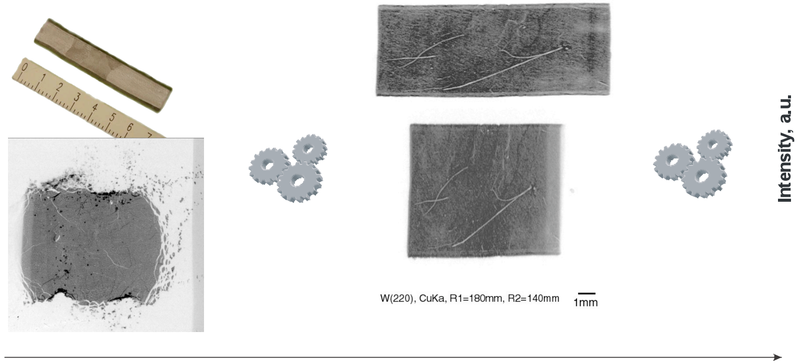

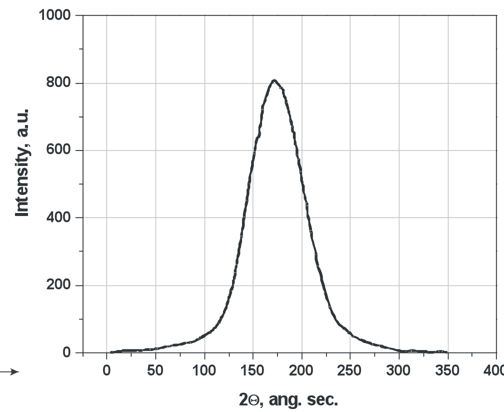

Recrystallized tungsten polycrystal and the angular scanning topogram. Angular scanning topograms of the samples W (110) after processing. The rocking curve.

Mosaicity is equal to 62”.

PXR in tungsten crystal with moderately relativistic carbon nucleus (γ=3.13)

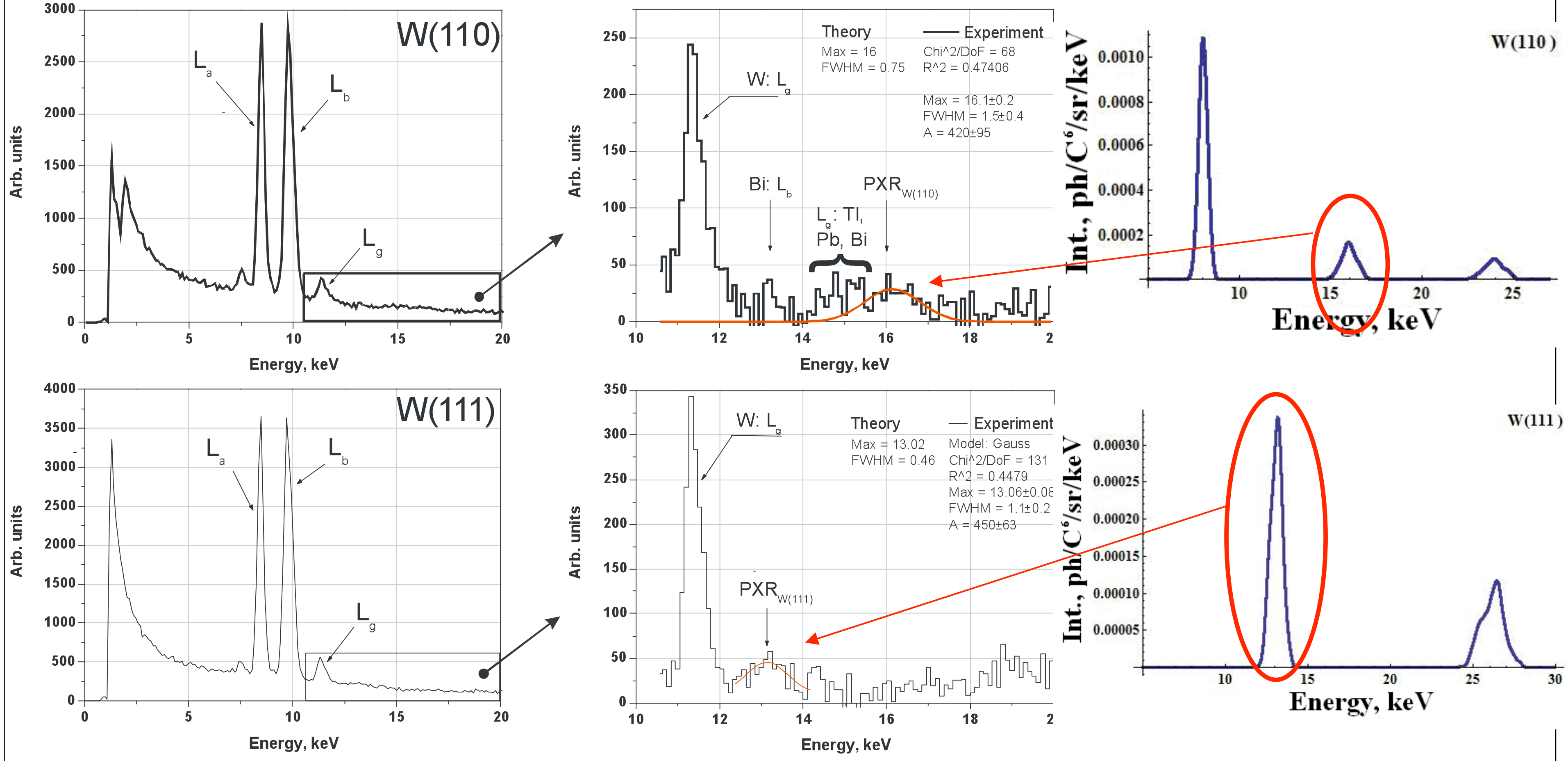

The spectra received with the experiment and the simulation are presented. Peaks of PXR was fitted with gauss. The maxima positions are 13.06±0.08 and 16.1±0.2 keV which correspond to calculation values of PXR lines from tungsten (111) and (110), accordingly.

PXR in tungsten crystal with moderately relativistic carbon nucleus (γ=3.13)

	Simulation		Experiment				
	hω, keV	Yied, ph/C^6/sr	hω, keV	N_c	N_γ	K_r	Yied, ph/C^6/sr
W (111)	13	$1.76 \cdot 10^{-4}$	13.06±0.08	$9 \cdot 10^{10}$	450±63	0.52	$(2.1 \pm 0.4) \cdot 10^{-4}$
W (110)	15.97	$9.12 \cdot 10^{-5}$	16.1±0.2	$8.3 \cdot 10^{10}$	420±95	0.35	$(2.5 \pm 0.7) \cdot 10^{-4}$

In according to simulation enhancement of yield in selected direction (observation angle 45°) is ~ 800% and 600% relative to the most strong reflection (11-1) for crystal W(111) and (02-2) in case W(110), respectively.

Case with mosaic crystal.

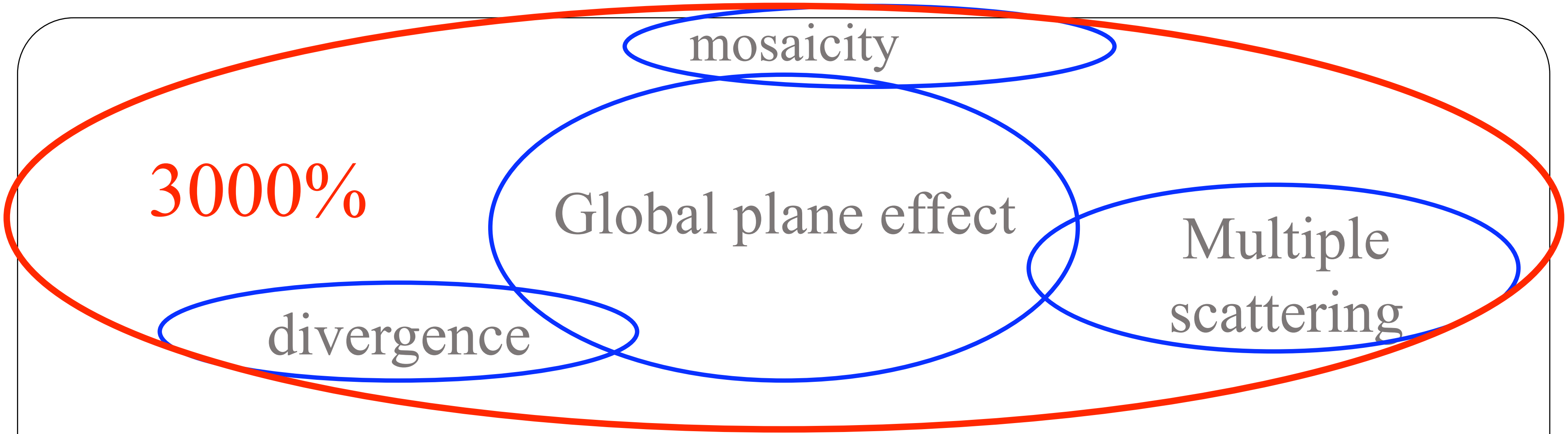

Simulation results of line shape of PXR generated with electrons with energy 5,6 MeV in tungsten crystal (111) with thickness 100 µm, are shown
Line width at energy 15,26 keV is $\Delta\omega = 1.57$ keV, at energy 30,54 keV – $\Delta\omega = 2.39$ keV for following parameters: beam divergence $\sigma_d = 5$ mrad, lateral dimension $\sigma_x = 1$ mm, $\sigma_y = 1$ mm, mosaicity $\sigma_m = 3$ mrad, detector apperture $d\Omega = 10^{-4}$sr . 1 m away from crystal.

(Int. ~10^{-5} ph/e$^-$/sr)

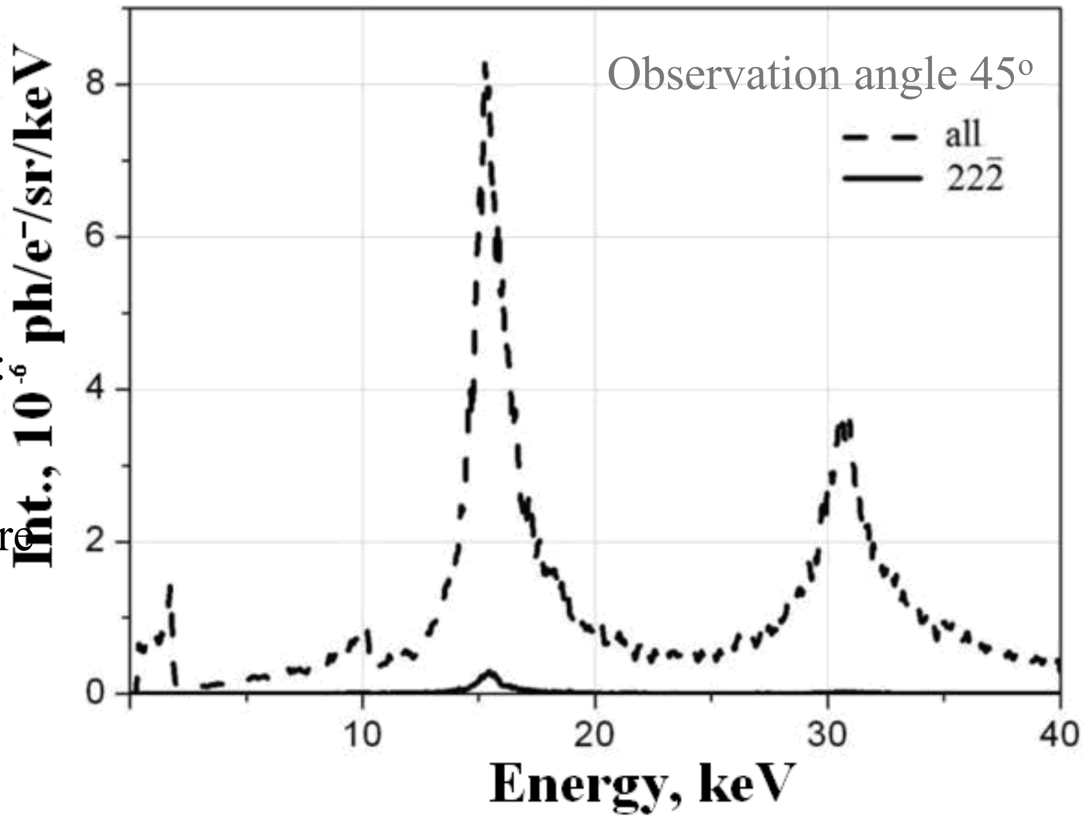

•Electron accelerator bremsstrahlung monochromatization

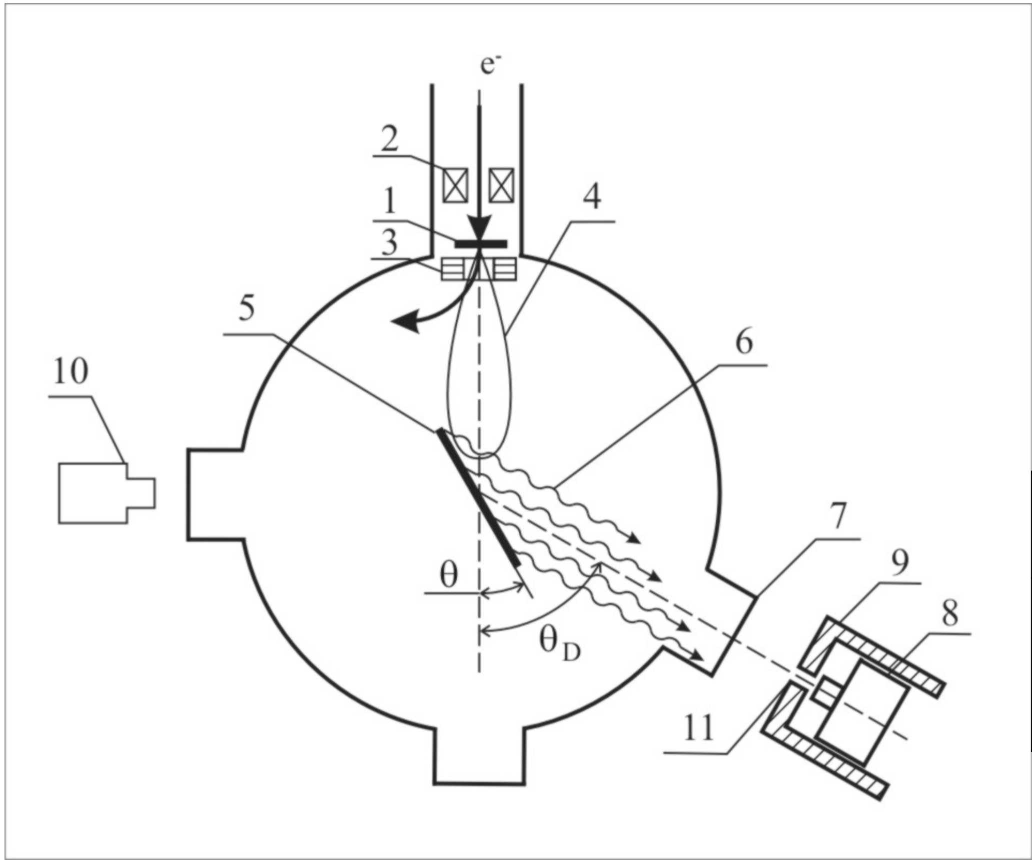

A.R. Wagner, A.P.Potylitsyn, et al., Monochromatic X-ray sources based on a mechanism of real and virtual photons diffraction in crystals, NIM **B** 266 (2008) 3893 - 3897

Electron energy	5.70 MeV
Beam current	0.15-0.30 mA

1 - aluminum converter (125 μm), 2 - current sensor, 3 - deflecting magnet, 4 - bremsstrahlung flux, 5 – crystal target fixed on goniometer, 6 - diffractions X-ray radiation, 7 - kapton window (150 μm), 8 - semiconductor silicon detector with a sensitivity region about 13 mm^2, 9 - lead chamber, 10 - TV-camera, 11 - collimator

Crystals parameters				
Parameters	C(002)	Ge(111)	W(111)	Unit
Linear dimensions	20×30	20 ×20	10×16	mm
Mosaicisity	~4	~1	~0,3	mrad
Thickness	350	2000	100	µm

•**Results of spectral measurements**

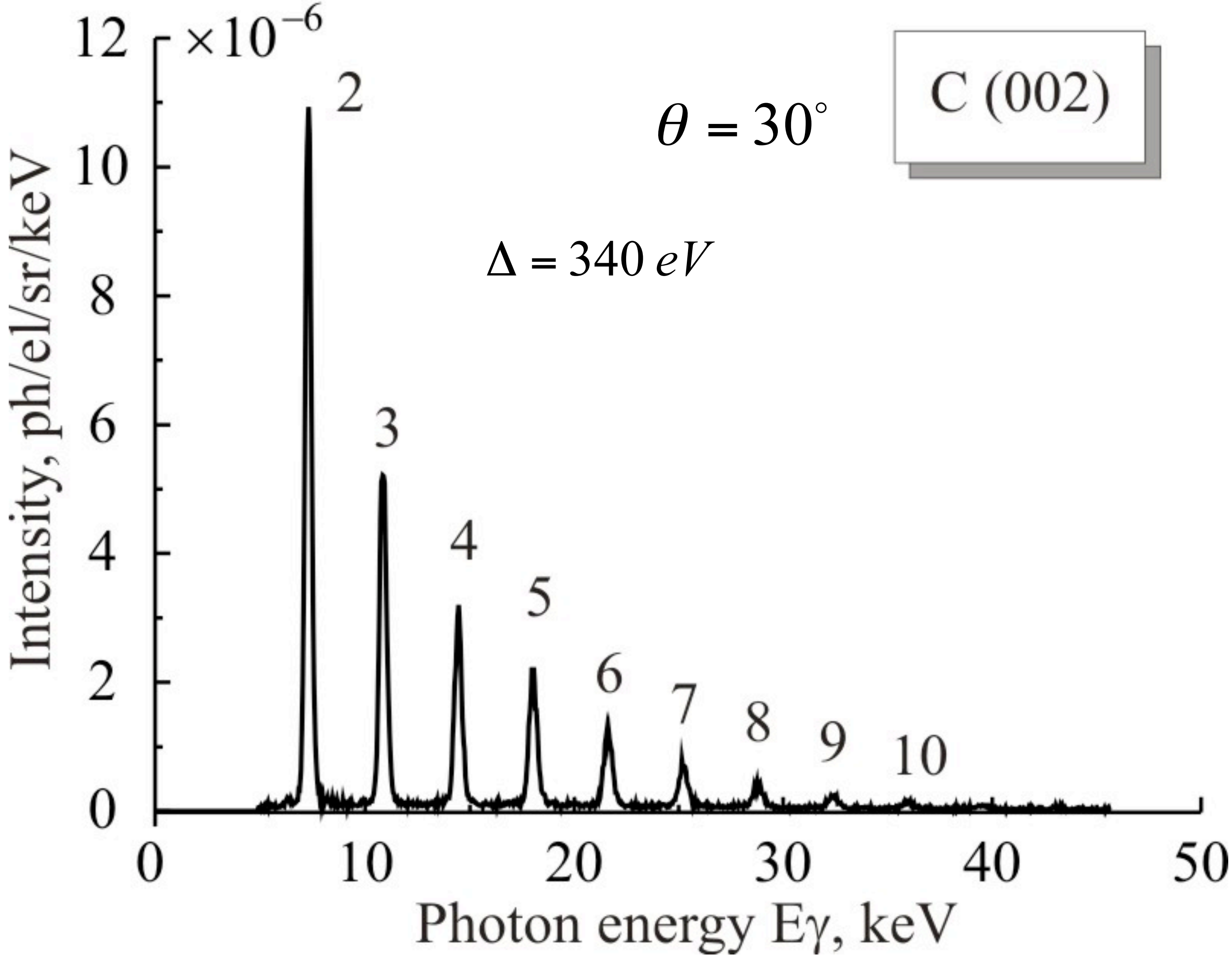

- **Characteristics of spectral line**

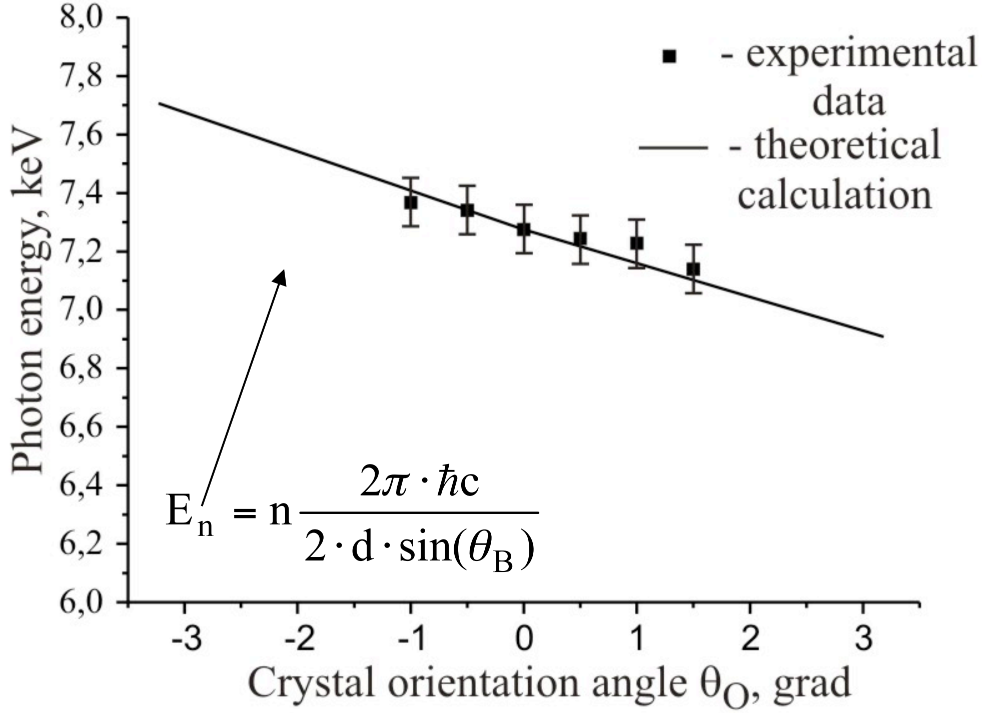

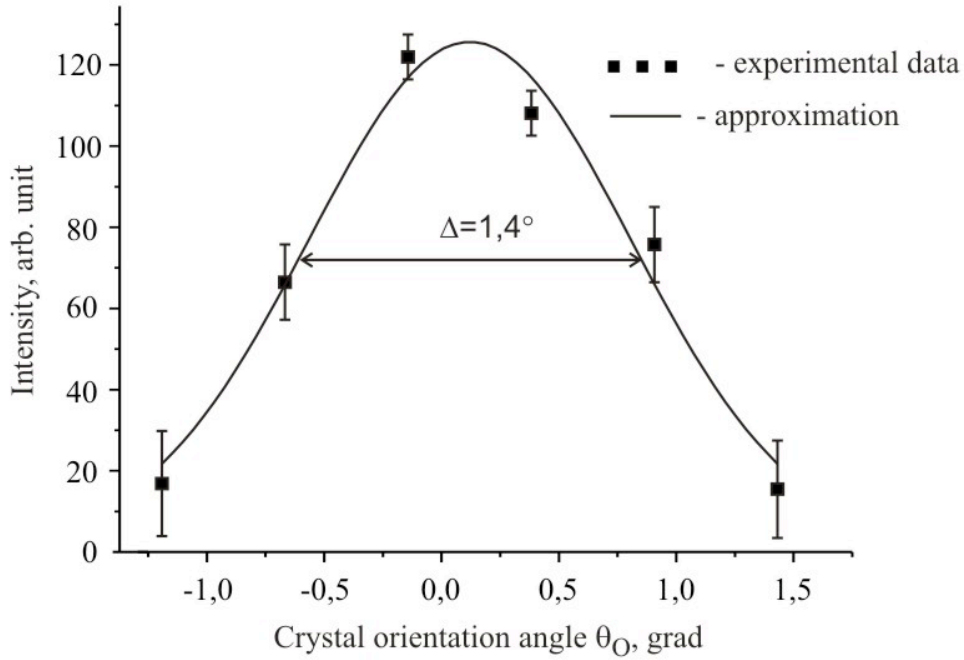

- **Comparison of DBS-lines with CXR ones**

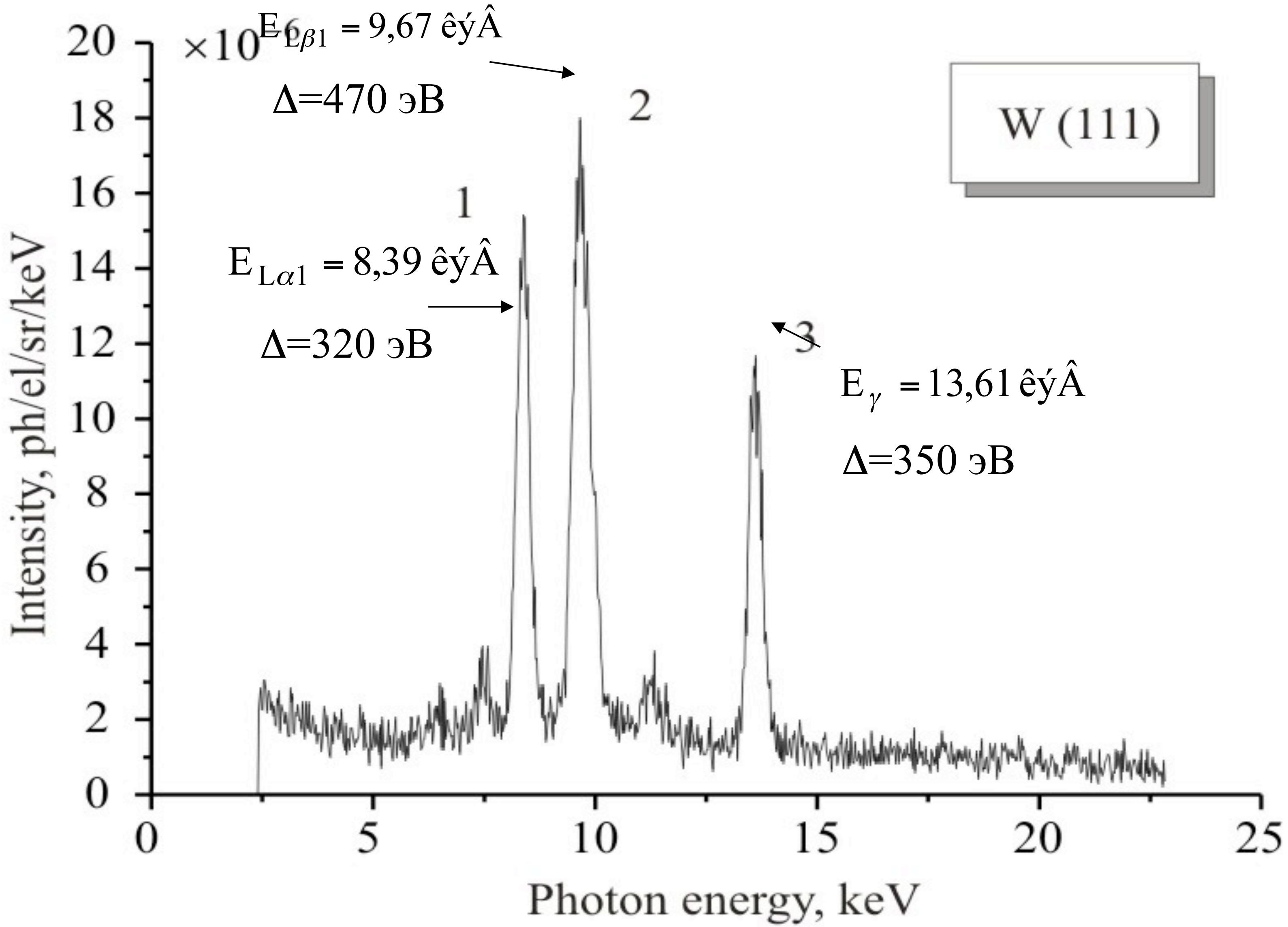

•**X-ray tube beam monochromatization by the same monochromator**

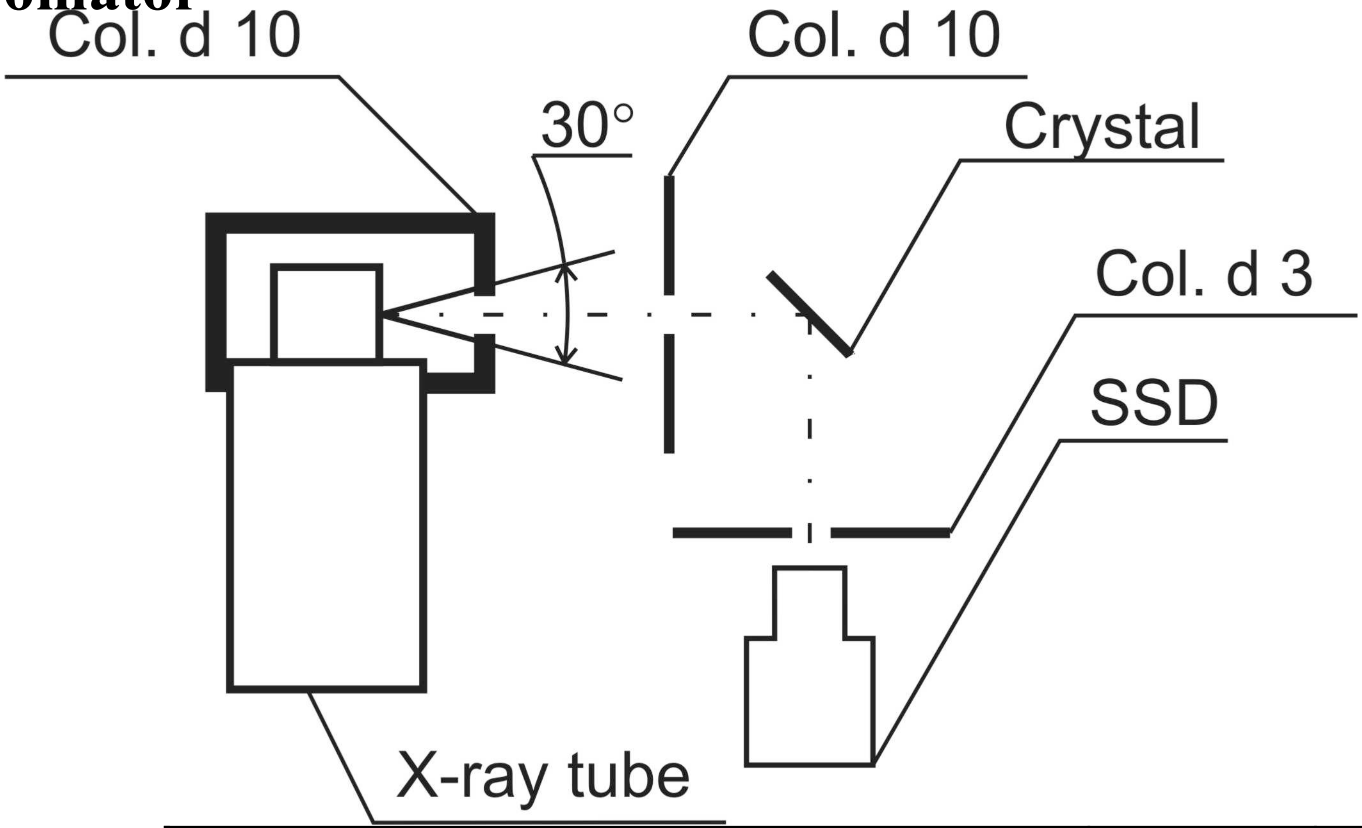

X-ray tube anode voltage	40	kV
X-ray tube anode current	10	mA
Anode material	Molybdenum	

•**X-ray tube spectrum**

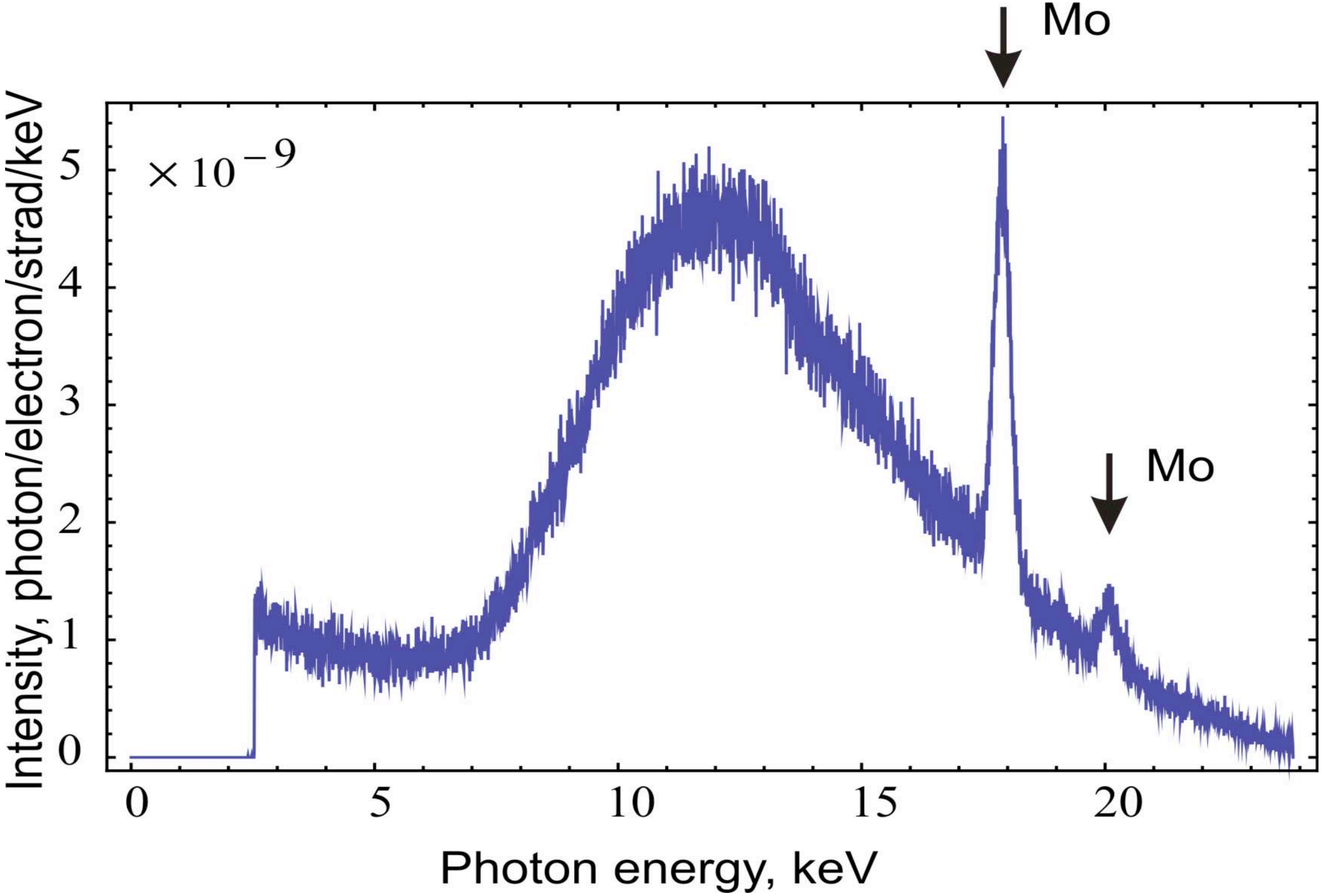

- **X-ray tube beam monochromatization**

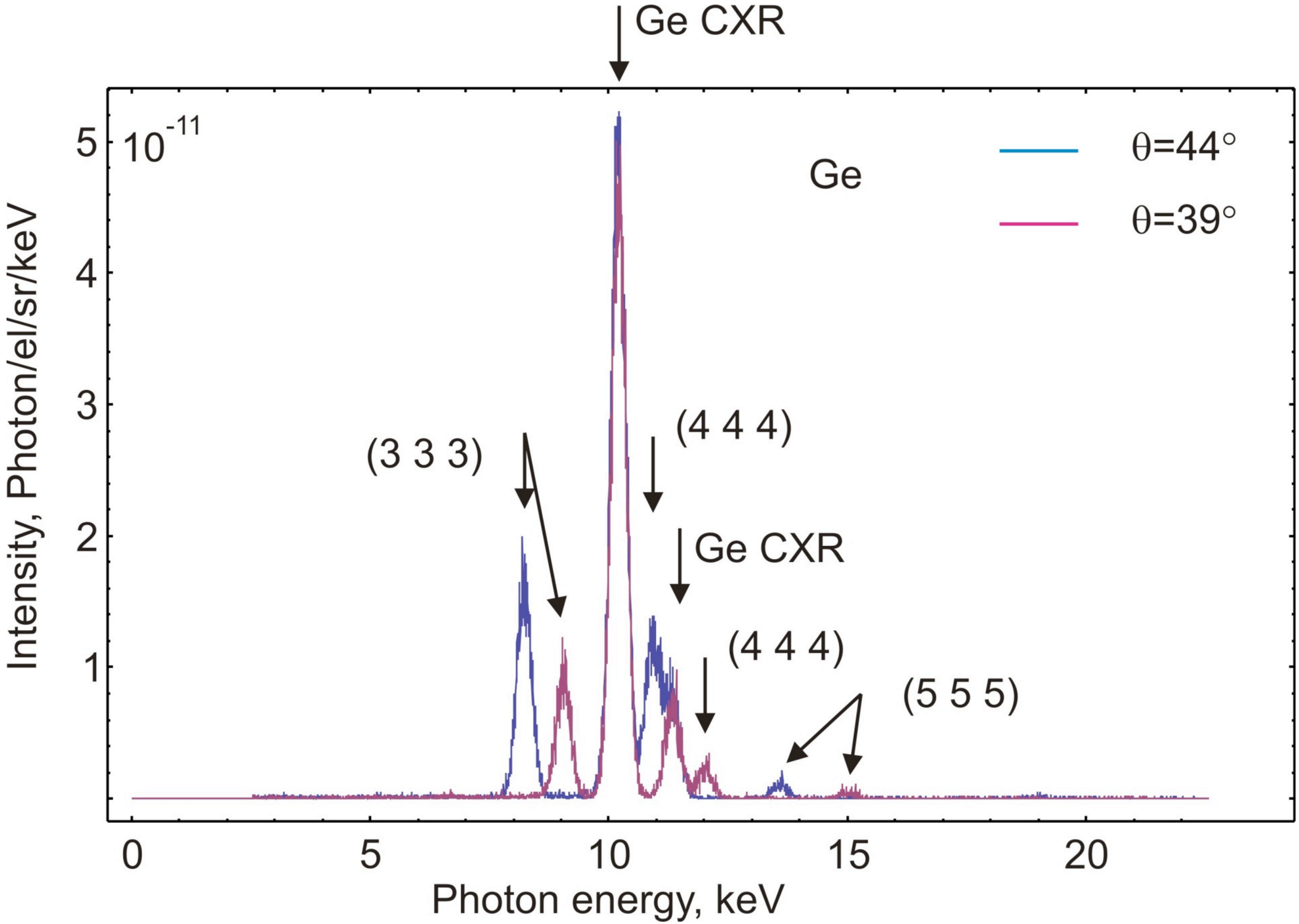

- **X-ray tube beam monochromatization**

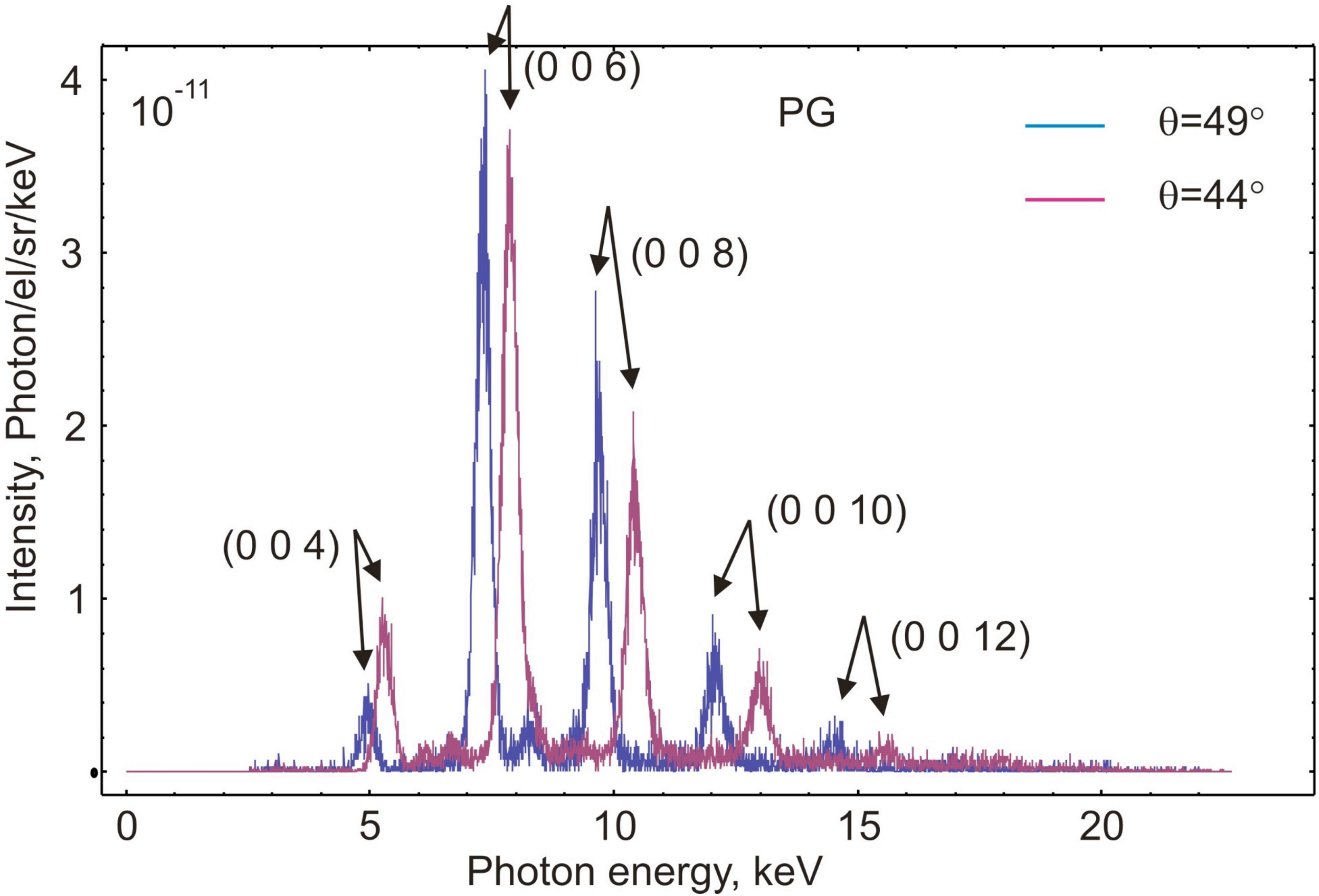

- **X-ray tube beam monochromatization**

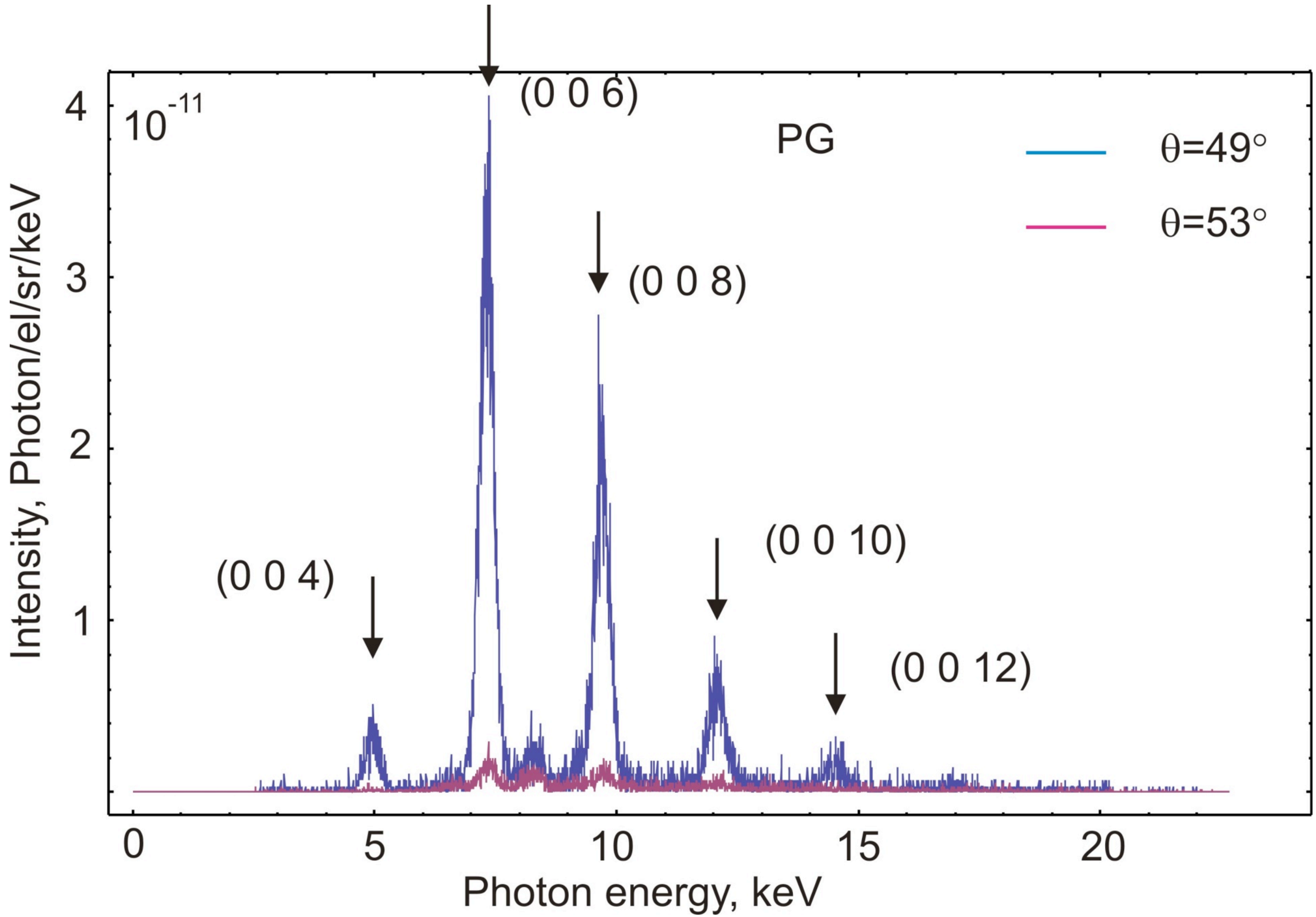

•Application and comparison

Microtron	0,3 mA	Pyrolytic graphite	7,29 keV	$8,5\cdot 10^{-6}$ $ph/el/sr$
X-ray tube	10 mA		7,9 keV	$1,3\cdot 10^{-11}$ $ph/el/sr$

The application of such source can be realize in radiography and angiography to improve an image contrast and to reduce a radiation dose obtained by patient.

The one image exposure time during coronary angiography is ~ 1 ms.

Microtron	0,6 μs	Pyrolytic graphite	$1,6\cdot 10^{10}$ ph/sr
X-ray tube	1 ms		$1,5\cdot 10^{3}$ ph/sr

•**Betatron 18 MeV**

Parameters

The maximum of electron energy	18	MeV
Frequency	150	Hz
Dose rate on 1 m distance	1 – 16	cGy/min
Focal point size	0,2 x 2	mm
Power	18	kW

Conclusion

•Electron accelerators with $E \leq 25$ MeV together with a monochromator may be considered as a simple and cheap device in order to obtain monochromatic X-ray sources

•RTR sources based on multilayer targets with submicrometer period have a good properties and should be investigated in future

•Use of superthin internal target ($t < 10^{-4}$ rad. length) in compact synchrotron or betatron allows to obtain high photon yield (due to multipass process) with narrow photon angular distribution $\sim\gamma^{-1}$

Conclusions

•Monochromatization of bremsstrahlung beam (or TR-beam) by external crystal-monochromator allows to obtain a spectral line with $\Delta E/E < 3\%$

•Enhancement of PXR yield due to global plane effect is shown from comparison our experiments and simulation results. Effect is revealed more intense for moderately relativistic particles ($\gamma < 10$, when angular distributions of PXR reflections are wide), mosaic crystals and divergent beams